STATISTICAL COMBINATION OF UNCERTAINTIES

PART 3

MARCH, 1980

POWER SYSTEMS
COMBUSTION ENGINEERING, INC.

LEGAL NOTICE

THIS REPORT WAS PREPARED AS AN ACCOUNT OF WORK SPONSORED BY COMBUSTION ENGINEERING, INC. NEITHER COMBUSTION ENGINEERING NOR ANY PERSON ACTING ON ITS BEHALF:

A. MAKES ANY WARRANTY OR REPRESENTATION, EXPRESS OR IMPLIED INCLUDING THE WARRANTIES OF FITNESS FOR A PARTICULAR PURPOSE OR MERCHANTABILITY, WITH RESPECT TO THE ACCURACY, COMPLETENESS, OR USEFULNESS OF THE INFORMATION CONTAINED IN THIS REPORT, OR THAT THE USE OF ANY INFORMATION, APPARATUS, METHOD, OR PROCESS DISCLOSED IN THIS REPORT MAY NOT INFRINGE PRIVATELY OWNED RIGHTS; OR

B. ASSUMES ANY LIABILITIES WITH RESPECT TO THE USE OF, OR FOR DAMAGES RESULTING FROM THE USE OF, ANY INFORMATION, APPARATUS, METHOD OR PROCESS DISCLOSED IN THIS REPORT.

CEN-124(B)-NP

STATISTICAL COMBINATION OF UNCERTAINTIES METHODOLOGY

PART 3:

C-E CALCULATED DEPARTURE FROM NUCLEATE BOILING AND LINEAR HEAT RATE LIMITING CONDITIONS FOR OPERATION FOR CALVERT CLIFFS UNITS 1 and 2

ABSTRACT

The three parts of the Statistical Combination of Uncertainties (SCU) report describe a method for statistically combining uncertainties involved in the calculation of the limits for the Reactor Protection and Monitoring Systems (RPS). Part 1 of the SCU report describes the application of these new methods for the development of the Local Power Density (LPD) and Thermal Margin/Low Pressure (TM/LP) Limiting Safety System Settings (LSSS's).Part 2 describes the statistical basis for a revised Departure from Nucleate Boiling Ratio (DNBR) corresponding to the Specified Acceptable Fuel Design Limit (SAFDL).

This part of the report, Part 3, describes the methods used to statistically combine uncertainties for the C-E calculated departure from nucleate boiling (DNB) and linear heat rate (LHR) limiting conditions for operation (LCO's).

Descriptions of the probability distributions of the LCO-related uncertainties and the stochastic simulation techniques developed for this program are presented. The total uncertainties presented in this report are expressed in percent overpower (P_{fdn}, P_{fdl}) units for the DNB and LHR LCO's respectively, at the 95% probability/95% confidence level limit.

Since the Required Overpower Margin (ROPM) is used to determine the LCO's, studies performed to determine the sensitivity of ROPM to these uncertainties are also discussed.

TABLE OF CONTENTS

TABLE OF CONTENTS (continued)

LIST OF TABLES

LIST OF FIGURES

LIST OF FIGURES (CONTINUED)

Definitions of Acronyms and Abbreviations

ACU	Axial shape index calibration uncertainty
AOO	Anticipated operational occurrence
APU	Axial shape index processing uncertainty
ARO	All rods out
ASI	Axial shape index
ASI_{DNB}	Axial shape index associated with P_{fdn}
ASI^{LCO}_{LHR}	Axial shape index associated with P^{LCO}_{fdl}
ASIU	Axial shape index units
B	Unless specifically defined in context as representing ΔT power, B is used as core power
B_1	Rod average power at which fuel design limit or DNBR is reached for initial steady state
B_2	Power at which fuel design limit on DNBR is reached for transient conditions
BASS	Better axial shape selection - a system used for in-core detector monitoring of the DNB LCO
B^{LCO}_{DNB}	Power level after inclusion of all DNB LCO uncertainties and allowances
BLIM	Allowable core power level in the BASS system
B^{LCO}_{LHR}	Power level after inclusion of the LHR LCO uncertainties and allowances
BMU	Power measurement uncertainty
BMU_K	Kth sampled value of BMU
BOL	Beginning of life
B_{OPM}	Available overpower margin
$\bar{B}_{OPM}$	Mean value of B_{OPM} distribution
B_{OPM_K}	The final B_{OPM} calculated from the Kth simulation trial
$B^{95/95}_{OPM}$	B_{OPM} at lower 95% probability/95% confidence level of B distribution

CEA	Control element assembly
CEAW	CEA withdrawal
CECOR	Computer code used to monitor core power distributions
CESEC	Computer code used to simulate NSSS response to perturbations
CETOP	Computer code used to determine the overpower limits due to thermal hydraulic conditions
CE-1	C-E's critical heat flux correlation
COAST	Computer code used to solve conservation equations for mass flow and momentum
CTM	Centerline temperature melt
DBE	Design basis event
DNB	Departure from nucleate boiling
DNBR	Departure from nucleate boiling ratio
f	Degrees of freedom
F_{aug}	Fuel-densitication-dependent power peaking augmentation factor
F	Primary coolant flow
F^{DNB}	Coolant flow used to evaluate the ordered pairs (P_{fdn}, Ip)
F^{LCO}	Flow component of the DNB LCO
FMU	Flow measurement uncertainty
F_q	Total 3D nuclear power peaking factor including the effect of augmentation factors
F_q^T	Total 3D nuclear power peaking factor including effects of tilt and augmentation factors
Fr	Integrated radial pin peaking factor
F_z	Core average axial power distribution peaking factor
FTC	Fuel temperature coefficient of reactivity
Fxy	Planar radial peaking factor
$\bar{I}_{PSINCA}$	Core average axial shape index calculated by the PSINCA program
I_1	Axial shape index of assembly i
$\bar{I}$	Core average axial shape index
$\bar{I}^R_{(r)}$	Rod position dependent core average axial shape index for ROCS calculated power shape
INCA	Computer code used to calculate power shapes from instrumented signals
Ip	Peripheral axial shape index
$I^R_p(r)$	Rod position dependent peripheral shape index for ROCS calculated power shape

$Ip^{RC(r)}$, $Ip^{RControl(r)}$	Rod configuration dependent peripheral shape index based on control channel assembly weighting factors
$Ip^{RS(r)}$, $Ip^{RSafety}$	Rod configuration dependent peripheral shape index based on safety channel assembly weighting factors
$(\bar{I}\text{-}Ip)^{ROCS}$	Difference between $\bar{I}$ and Ip for a ROCS calculated power distribution
$(\bar{I}\text{-}Ip)^{CECOR}$	Difference between $\bar{I}$ and Ip for a CECOR evaluated power distribution
$(Ip^{ROCS}\text{-}Ip^{CECOR})_{Safety}$	Difference between ROCS and CECOR calculated Ip using the safety channel assembly weighting factors
$(Ip^{ROCS}\text{-}Ip^{CECOR})_{Control}$	Difference between ROCS and CECOR calculated Ip using the control channel assembly weighting factors
k	Stochastic simulation trial number
K	One-sided tolerance factor at the 95% probability/ 95% confidence limit
LCO	Limiting condition for operation
LHR	Linear heat rate
LOF	Loss of flow
LPD	Local power density, also known as axial flux offset
LSSS	Limiting safety system setting
MTC	Moderator temperature coefficient
n	Normal distribution
N	Total number of sampled cases in DNB LCO uncertainty analyses
NA	Not applicable
NSSS	Nuclear steam supply system
P	Pressurizer pressure
P_i	Axial integrated power of assembly i
P_1	Initial power level in CEA drop event analysis
P_2	Final power level in CEA drop event analysis
P^{DNB}	System pressure used in the calculation of the ordered pairs (P_{fdn}, Ip)
PSINCA	Computer code used to calculate $\bar{I}_{PSINCA}$ and BLIM for in-core monitoring of DNB LCO

P_{fdl}	Power to fuel design limit on linear heat rate
P_{fdl}^{LCO}	P_{fdl} for LHR LCO including effects of azimuthal tilt
P'_{fdl}	P_{fdl} for LHR LCO not including the effects of azimuthal tilt
P_{fdn}	Power to fuel design limit on DNB including the effects of azimuthal tilt
P'_{fdn}	Power to fuel design limit on DNB
P_{fdn_k}	Overpower from the kth simulation trial CETOP calculation
p^{LCO}	Pressure component of the DNB LCO
PLCS	Pressurization level control system
PLHGR	Peak linear heat generation rate
PPCS	Pressurization pressure control system
PMU	Pressure measurement uncertainty
PU	Uncertainty in predicting local power at the fuel design limit
QUIX	Computer code for solving the one-dimensional diffusion equations
RCS	Reactor coolant system
ROCS	Coarse mesh code for calculating power distributions
ROPM	Required overpower margin
RPS	Reactor protection system
RSU	Shape index separability uncertainty
RTD	Resistance temperature devices
SAFDL	Specified acceptable fuel design limit
SAU	Shape annealing factor uncertainty
SC	Approved credit in lieu of statistical combination of uncertainties
SCU	Statistical combination of uncertainties
SIGMA	Stochastic simulation code
SMDO	Statistically combined uncertainty applicable to the DNB LCO
SMLO	Statistically combined uncertainty applicable to the LHR LCO
STRIKIN	Computer code used to calculate fuel rod heat transfer

T_{AZ}	Azimuthal tilt allowance
T_c	Primary coolant inlet temperature, cold leg temperature
T_h	Primary coolant hot leg temperature
T_{in}^{DNB}	Inlet coolant temperature used in calculating the ordered pairs (Pfdn, Ip)
T_{in}^{LCO}	Inlet temperature for the DNB LCO
$T_{in}^{LCO,DNB}$	Inlet temperature for the DNB LCO after accounting for the temperature measurement uncertainty
TM/LP	Thermal margin/low pressure
TMU	Temperature measurement uncertainty
TORC	Code for calculating thermal hydraulic response to variations of system variables
TORC/CE-1	Thermal hydraulic calculational model including CE-1 critical heat flux correlation
W_{avg}	Core average linear heat rate
W_i^j	Weighting factor of assembly i for excore detector set j
W_{max}^{LCO}	Maximum linear heat rate limit allowed by the LHR LCO
α	Shape annealing factor
ΔB_{OPM_k}	kth sampled overpower uncertainty due to ASI uncertainties
ΔI_{p_1}	Uncertainty in Ip due to uncertainty components other than electronic processing
ΔI_{p_2}	Uncertainty in Ip due to electronic processing
ΔP	Pressure difference
ΔT	Temperature difference
μ	Axial shape index correction term
μ_C	[ ]
μ_R	[ ]
$\mu_{Q(r)}$	[ ]
μ_R^{SC}	[ ]
μ_S	[ ]
σ	Standard deviation

1.0 INTRODUCTION

1.1 PURPOSE

Part 1 of the SCU report[1-1] describes the application of C-E's method for statistically combining the uncertainties involved in the calculation of the limits for the local power density and thermal margin/low pressure limiting safety system settings (LSSS). Part 2[1-2] describes the statistical basis for the revised departure from nucleate boiling ratio (DNBR) limit to be used in the evaluation of LSSS's and limiting conditions for operation (LCO's).

The purpose of Part 3 of the report is to describe the method for statistically combining the uncertainties involved in the calculation of the limits for the DNB and LHR LCO's. Uncertainties for the variables listed in Table 1-1 are considered.

1.2 BACKGROUND

1.2.1 Protection and Monitoring System

The basic purposes and interactions of the LSSS and LCO's were previously described in Section 1.2.1 of Part 1 of this report. Part 1 describes the function of the protection system; Part 3 describes the function of the DNB and LHR LCO's.

Operation within the DNB and LHR LCO's provides the necessary initial DNB and LHR margin to prevent exceeding acceptable limits during Design Basis Events (DBE's) where changes in DNBR and linear heat rate are important. A list of the Nuclear Steam Supply System (NSSS) parameters which affect the calculation of these LCO's is shown in Table 1-2. A discussion of C-E setpoint methodology may be found in Reference 1-3.

Either the ex-core or the in-core detectors can be used to monitor the LHR LCO for C-E designed reactors. For Calvert Cliffs Units 1 and 2, the DNB LCO and axial shape index can now be monitored on in-core detectors as well as on the ex-core detectors. This use of in-core detectors is described in Reference 1-4. Although these two DNB LCO monitoring systems are functionally similar in that they correlate allowed power levels and axial shape indices, use of the in-core detectors rather than the ex-core detectors implies different[

] These differences are noted herein.

1.2.2 Previous Uncertainty Evaluation Procedure

The methods previously used to apply uncertainties to generate DNB and LHR LCO's are presented in Reference 1-3 and are summarized in Appendix B.

As noted in Reference 1-3, these methods assume that all applicable uncertainties occur simultaneously in the most adverse direction. This assumption is conservative. Not all of the uncertainties are systematic; some are random and some contain both systematic and random components. As described in References 1-5,1-6. partial credit for statistical combination of uncertainties has been allowed for the DNB LCO in view of the existence of this conservatism. This report documents the methodology used to statistically combine the LCO-related uncertainties explicitly, in lieu of the credit previously used.

1.2.3 Design Basis Event Transient Analysis Evaluation

The methods and procedures used in the report to analyze DBE's were approved by NRC in References 1-7 and 1-8. The purpose of the transient analysis evaluations is to determine the sensitivity of and variation in the required overpower margin due to the way the uncertainties are treated.

1.3 REPORT SCOPE

The scope of this part of the SCU report encompasses the following objectives:

1. To define the methods used to statistically combine uncertainties applicable to the calculation of the DNB and LHR LCO's

2. To determine the aggregate uncertainties as they are applied in the determination of the DNB and LHR LCO's

3. To determine whether statistically combined uncertainties affect the selection of initial conditions for the transient analyses of DBE's and to determine the magnitude of variations of ROPM within the range of the uncertainties of the key parameters.

One requirement for achieving the objectives is to define the probability distributions associated with the uncertainties being considered. The development of those distributions which impact the LCO's differently than they impacted the LSSS's is discussed in Appendix A. To achieve the third objective, it is necessary to examine the sensitivity of ROPM to initial conditions for DNB and LHR-related DBE's. These evaluations are discussed in Appendix C.

The methods presented in this report are applicable specifically to the 4-pump operation of the Calvert Cliffs Units 1 and 2 (Baltimore Gas & Electric) reactors.

1.4 SUMMARY OF RESULTS

The analytical methods presented in Section 2.0 are used to show that a stochastic simulation of uncertainties associated with the ex-core detector-monitored DNB and LHR LCO's results in aggregate uncertainties of [ ] respectively, at a 95/95 probability/confidence level. The total uncertainties previously applied to the ex-core DNB and LHR LCO's are approximately [ ] respectively. Therefore, the statistical combination of uncertainties program provides a reduction in the conservatism of the uncertainties applied in establishing the ex-core instrument monitored DNB and LHR LCO's of approximately [ ], respectively. The stochastic simulation of uncertainties associated with in-core monitoring of the DNB LCO results in an aggregate uncertainty of [ ] at the 95/95 probability/confidence level.

The DBE sensitivity evaluations, described in Appendix C, show that the required overpower margin used in LCO generation is insensitive to the way uncertainties are combined.

1.5 REFERENCES FOR SECTION 1

1-1 CEN-124(B)-P, Statistical Combination of Uncertainties, Part 1, December 1979

1-2 CEN-124(B)-P, Statistical Combination of Uncertainties, Part 2, January 1980

1-3 CENPD-199-P, C-E Setpoint Methodology, April 1976

1-4 CEN-119(B)-P, BASS , November 1979

1-5 Docket No. 50-317, Safety Evaluation by the Office of Nuclear Reactor Regulation for Calvert Cliffs Unit 1 Cycle 3 , June 30, 1978

1-6 Docket No. 50-318, Letter R. R. Reid (NRC) to A. E. Lundvall, Jr. (BG&E), License Amendment No. 18 and SER for Calvert Cliffs Unit No. 2, October 21, 1978

REFERENCES FOR SECTION 1 (continued)

1-7 Letter, D. L. Zieman (NRC) to A. E. Lundvall, Jr. (BG&E) dated March 14, 1977, License Amendment 21 and SER for Cycle 2 Operation of Calvert Cliffs Unit 1. Docket No. 50-317

1-8 Letter, R. W. Reid (NRC) to W. G. Counsil (NNEC) dated May 12, 1979, License Amendment 52 and SER for Cycle 3 Operation of Millstone Point Unit 2. Docket No. 50-336

TABLE 1-1

VARIABLES AFFECTING THE LCO-RELATED UNCERTAINTIES

1. Predicted integrated radial pin power at the fuel design limit
2. Power measurement
3. Shape annealing factor
4. Shape index separability
5. Axial shape index calibration
6. Equipment processing of detector signals
7. Flow measurement
8. Pressure measurement
9. Temperature measurement

TABLE 1-2

"SSS PARAMETERS AFFECTING THE DNB AND LHR LCO's

DNB

1. Core Power
2. Axial Power Distribution
3. Radial Power Distribution
4. Azimuthal Tilt Magnitude
5. Core Coolant Inlet Temperature
6. Primary Coolant Pressure
7. Primary Coolant Mass Flow

LINEAR HEAT RATE

1. Core Power
2. Axial Power Distribution
3. Radial Power Distribution
4. Azimuthal Tilt Magnitude

2.0 ANALYSES

2.1 GENERAL

The following sections provide a description of the analyses performed to statistically combine uncertainties associated with the DNB and LHR LCO's. The statistical combination technique involves use of the computer code SIGMA (Reference 2-1) to select data for the stochastic simulation of the DNB and LHR LCO calculations. The bases for the individual uncertainties not previously described in Part 1 (Reference 2-2) are presented in Appendix A. The stochastic simulation techniques are described below.

2.2 OBJECTIVES OF ANALYSES

The objectives of the analyses presented in this section are

1. To document the stochastic simulation techniques for the uncertainties associated with parameters that affect the LHR and the DNB LCO's

2. To determine the 95/95 probability/confidence level uncertainty factors to be applied in calculating the LHR and DNB LCO's

2.3 ANALYSIS TECHNIQUES

2.3.1 General Strategy

The stochastic simulation code used for the statistical combination of the DNB and LHR LCO related uncertainties is the computer code SIGMA. It is described in Section 2.3.1 of Part 1 of this report (2-2).

2.3.2 DNB LCO Stochastic Simulation

For the DNB LCO, DNB overpower (P_{fdn}) divided by the required overpower margin (ROPM) is the dependent variable of interest. The core coolant inlet temperature, reactor coolant system pressure and flow rate, peripheral axial shape index and integrated radial peaking factor are the independent variables of interest. As demonstrated in Appendix C, ROPM is relatively insensitive to these independent variables. In addition, the maximum ROPM as a function of shape index is used as input to generate the LCO's. This reduces the analytical evaluation of the dependent variable to consideration of the Pfdn's response to the uncertainties of the independent variables. TORC/CE-1 (References 2-3, 2-4) is used to determine the functional relationship between P_{fdn} and the independent variables. The probability distribution of uncertainties associated with some of the independent variables have been discussed in Appendix A of Part 1 of this report. Those uncertainties specifically associated with the calculation of the core average axial shape index using the in-core detector system to monitor the the DNB LCO (Reference 2-5) are discussed in Appendix A of this part of the report.

The core coolant inlet temperature range of interest for the DNB LCO stochastic simulation is defined by:

(1) the temperature at which the secondary safety valves open, and

(2) the temperature at which the low secondary pressure trip would occur.

The reactor coolant system pressure range of interest for the DNB LCO stochastic simulation is defined by:

(1) the value of the high pressurizer pressure trip setpoint, and

(2) the lower pressure limit of the thermal margin/low pressure trip.

It is noted that these ranges are the same as used in the LSSS stochastic simulation (Ref. 2-2) and as such are bounding for the LCO.

Figure 2-1 is a flow chart representing the ex-core detector monitoring stochastic simulation of the DNB limits. This figure is similar to Figure 2-2 in Part 1. Figure 2-2 is a flow chart representing the in-core detector monitoring stochastic simulation of the DNB limits. This figure differs from Figure 2-1 in that the

[ ]stochastic simulation. The independent variables and their uncertainties are input to SIGMA. Each data set generated by SIGMA is evaluated with TORC/CE-1 to generate a P_{fdn} probability distribution. The ratio of the mean value of P_{fdn} to the lower 95/95 value of P_{fdn} is the parameter of interest. The details of the specific DNB LCO stochastic simulations performed are presented in Section 2.4.

2.3.3 LHR LCO Stochastic Simulation

For the LHR LCO, the LHR LCO overpower (P_{fdl}^{LCO}) is the dependent variable of interest. The three-dimensional (3D) pin power peak, the core average power level and the peripheral axial shape index are the independent variables. The dependent variable is defined as

$$P_{fdl}^{LCO} = \frac{W_{max}^{LCO} \times 100}{W_{avg} \times F_q^T} \qquad (2\text{-}1)$$

where W_{max}^{LCO} is the peak linear heat rate allowed by the LHR LCO and is determined by analysis of DBE's.

W_{avg} is the core average generated linear heat rate at rated power

F_q^T is the synthesized core power peak including the effects of azimuthal tilting and augmented power peaking due to fuel densification.

In all other ways, the stochastic simulation procedure for the LHR LCO is the same as the simulation procedure for the LPD LSSS described in Section 2.3.3 of Part 1.

2.4 ANALYSES PERFORMED

2.4.1 DNB LCO Uncertainty Analysis

Evaluation of the combination of uncertainties for the DNB LCO is similar to the TM/LP LSSS analysis reported in Part 1. The distributions of the uncertainties of the following parameters are input to the analysis:

[ ]

In order to combine the significant uncertainties in the same manner as shown in Figure 2-1 of Part 1, the LCO stochastic simulation sequence shown in Figure 2-1 of Part 3 was used.

2.4.1.1 Simulation Module SIGMA

The simulation process is carried out over all of the operating space, defined in Section 2.3.2, in the same manner as described in Section 2.4.1.1 of Part 1.

2.4.1.2 Axial Shape Index Uncertainty Simulation

2.4.1.2.1 Ex-Core Axial Shape Index

The basic relationships between the components of the ex-core safety channel monitored axial shape index uncertainty for LSSS were described in Appendix A1 of Part 1. However, only the set of ex-core detectors designated as "control channels" supply information for the calculation of the axial shape index used to monitor the LCO on power versus shape index. As shown in Figure 2-3, the location of the control channel ex-core detectors relative to the reactor cavity are similar to the locations of the safety channels.
Because the core is sited with one of its main diameters aligned with the cavity's north/south line (Reference 2-5), the ex-core detector uncertainty's

dependence on position is the same for the control channels as it was for the safety channels. However, the circuitry for the control channel shape index evaluation is different from the circuitry for the safety channel shape index evaluation. This circuitry difference is incorporated with the electronic processing simulator of the stochastic simulation for the DNB LCO (Figure 2-1). Thus, except for the processing uncertainty component, the shape index uncertainties developed in Appendix A1 of Part 1 are appropriate for the LCO simulations.

2.4.1.2.2 Core Average Axial Shape Index

The uncertainties associated with the in-core detector system have been developed in support of the better axial shape selection system (Reference 2-6). The magnitude of those uncertainties are defined in Appendix A of this part of the report.

The procedure used to sample the shape index uncertainty distributions for the LCO stochastic simulation are those described in Section 2.4.1.2 of Part 1.

2.4.1.3 Processing Uncertainty Simulation

2.4.1.3.1 Ex-Core Instrument Processing

As in the LSSS analysis described in Part 1, the signals generated by the ex-core detectors are processed into a power and an axial shape index (ASI) value. The electronic processing equipment introduces further uncertainty in these values. Since the axial power distribution and the ASI value used in each simulation calculation are correlated, this uncertainty is incorporated in the stochastic evaluation of the LCO.

2.4.1.3.2 In-Core Instrument Processing

As noted in Appendix A the processing uncertainty for the in-core instrument signals has been [

]

2.4.1.4 Overpower Calculation With Respect to DNB LCO

As in Part 1, the overpower limits due to reactor thermal-hydraulic conditions are determined by the code CETOP (Reference 2-7), which uses the CE-1 correlation. CETOP requires values of the pressure, inlet temperature, average coolant mass flow, and radial peaking factor, and calculates a limit on overpower.

2.4.1.5 Combination of Uncertainties

As in Part 1, during each simulation trial(k),a calculation is performed to determine the ratio of the value of overpower at nominal (mean) conditions to the value at off-nominal conditions as the result of sampling values from the appropriate uncertainty distributions. These uncertainties are combined by using the following relations:

[ ] 2-2

where [ ]

2.4.2 LHR LCO Uncertainty Analysis

The stochastic simulation calculation used for the LPD LSSS uncertainty analysis in Section 2.4.2 of Part 1 was repeated for the LHR LCO uncertainty analysis with only minor changes. In the simulations, the overpower (P_{fdl}^{LCO}) is derived from the technical specification value of the LHR LCO limit.

The axial shape index uncertainty and the processing uncertainty simulations of Sections 2.4.1.2 and 2.4.1.3 were also applied to this analysis.

2.5 REFERENCES FOR SECTION 2

2-1 F. J. Berte, "The Application of Monte Carlo and Bayesian Probability Techniques to Flow Prediction and Determination", TIS-5122, February 1977

2-2 CEN-124(B)-P, "Statistical Combination of Uncertainties Part 1", December 1979

2-3 CENPD-161-P, "TORC Code: A Computer Code for Determining the Thermal Margin of a Reactor Core", July 1975

2-4 CENPD-206-P, "TORC Code: Verification and Simplified Modeling Methods", January 1977

2-5 Calvert Cliffs Units 1 and 2 FSAR

2-6 CEN-119(B)-P, "BASS", November 1979

2-7 C. Chiu, J. F. Church, "Three-Dimensional Lumped Subchannel Model and Prediction-Correction Numerical Method for Thermal Margin Analysis of PWR Cores", TIS-6191, June 1979

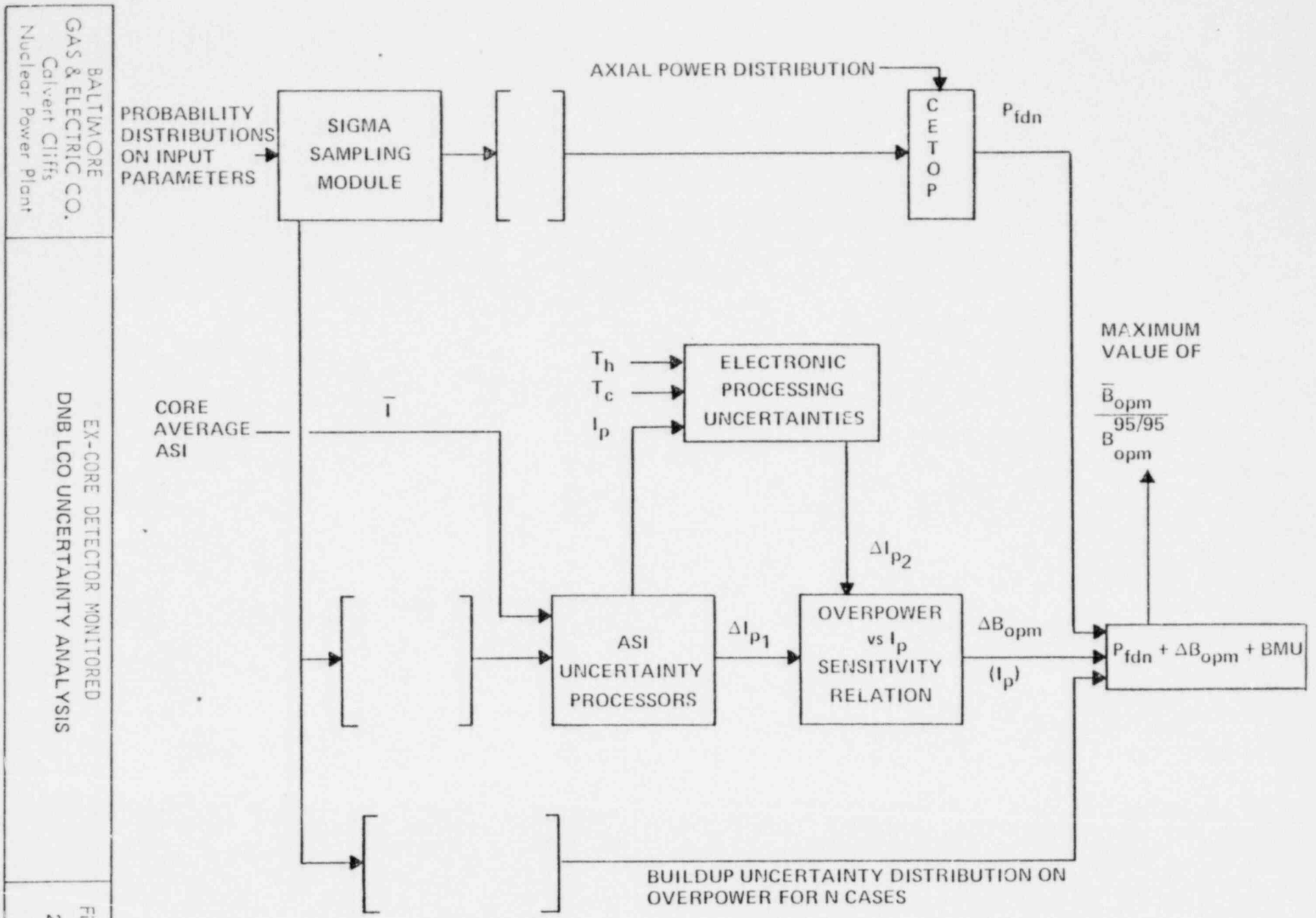
BALTIMORE GAS & ELECTRIC CO.
Calvert Cliffs Nuclear Power Plant
EX-CORE DETECTOR MONITORED DNB LCO UNCERTAINTY ANALYSIS
Figure 2-1
PROBABILITY DISTRIBUTIONS ON INPUT PARAMETERS
SIGMA SAMPLING MODULE
AXIAL POWER DISTRIBUTION
C E T O P
P_{fdn}
MAXIMUM VALUE OF
$\frac{\bar{B}_{opm}}{B_{opm}^{95/95}}$
T_h
T_c
I_p
ELECTRONIC PROCESSING UNCERTAINTIES
CORE AVERAGE ASI
$\bar{I}$
ΔI_{p2}
ASI UNCERTAINTY PROCESSORS
ΔI_{p1}
OVERPOWER vs I_p SENSITIVITY RELATION
ΔB_{opm}
(I_p)
$P_{fdn} + \Delta B_{opm} + BMU$
BUILDUP UNCERTAINTY DISTRIBUTION ON OVERPOWER FOR N CASES

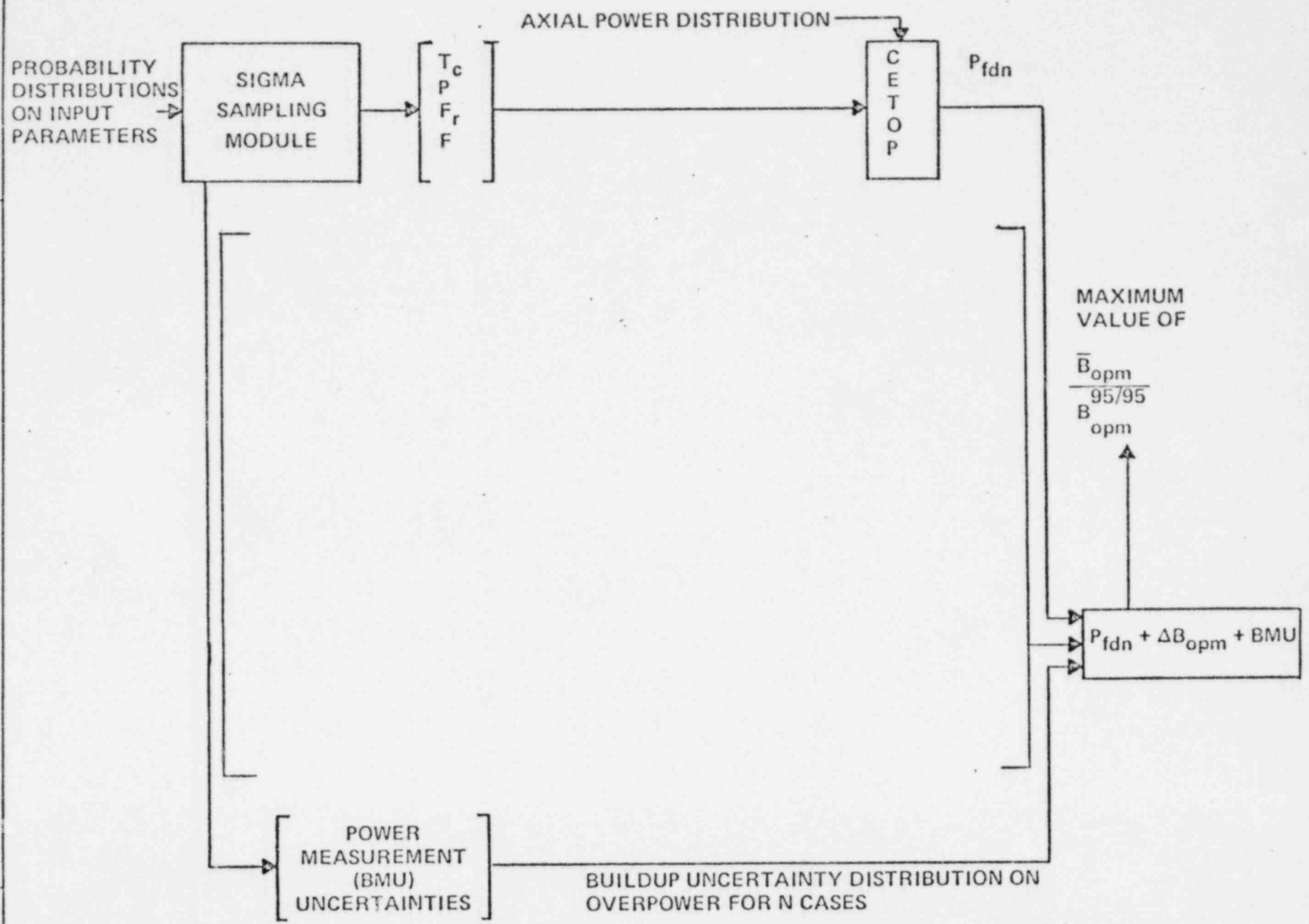

BALTIMORE GAS & ELECTRIC CO.
Calvert Cliffs Nuclear Power Plant

IN-CORE DETECTOR MONITORED DNB LCO UNCERTAINTY ANALYSIS

Figure 2-2

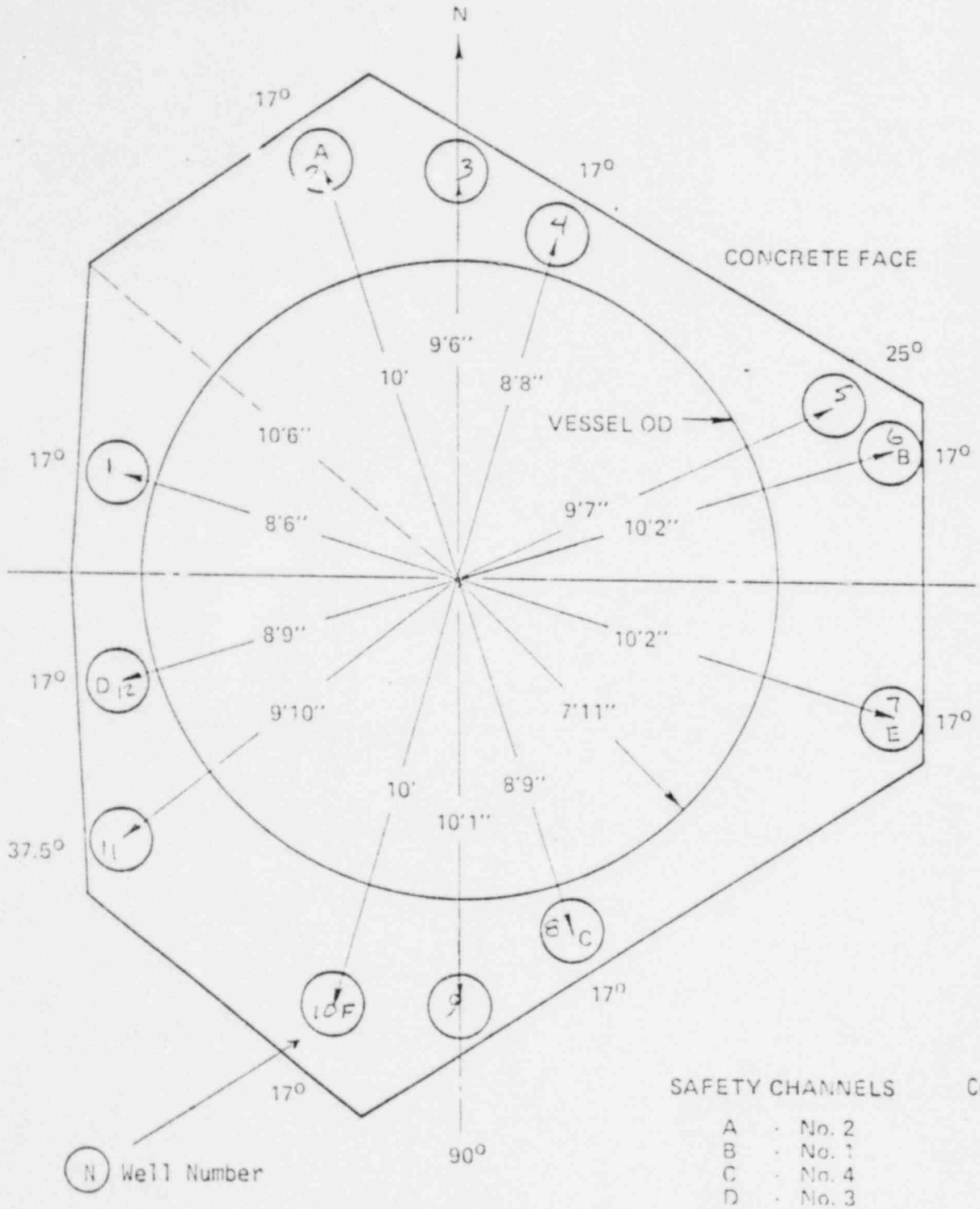

SAFETY CHANNELS	Control Channels
A - No. 2	E
B - No. 1	F
C - No. 4	
D - No. 3	

BALTIMORE GAS & ELECTRIC CO. Calvert Cliffs Nuclear Power Plant	REACTOR CAVITY CROSS-SECTION AND EX-CORE DETECTOR LOCATION	Figure 2-3

3.0 RESULTS AND CONCLUSIONS

3.1 RESULTS OF ANALYSES

The statistical analytical methods presented in Section 2 have been used to show that a stochastic simulation of uncertainties associated with the ex-core monitored DNB and LHR LCO's result in aggregate uncertainties of [ ], respectively, at a 95/95 probability/confidence level. Stochastic simulation of the in-core monitored DNB LCO results in an aggregate uncertainty of [ ].

Table 3-1 shows the values of the individual uncertainties which were statistically combined to yield the above aggregates. Appendix A contains a further discussion of the bases for these individual uncertainties.

The aggregate uncertainties are in units of percent overpower (P_{fdn}, P_{fdl}) and are applied as such in the generation of the LCO limits as discussed below.

3.1.1 DNB LCO

The fuel design limit on DNBR for the DNB LCO is represented by a combination of the ordered pairs (P_{fdn}, ASI_{DNB}). A lower bound is drawn under the "flyspeck" data such that all the core power distributions analyzed are bounded. This lower bound is reduced by applicable uncertainties as follows:

[ ]

(3-1)

(3-2)

(3-3)

where:

B_{DNB}^{LCO} - DNB power limit for LCO after inclusion of uncertainties and allowances

P_{fdn} - Power to fuel design limit on DNB including the effects of azimuthal tilt

SMDO - Statistically combined uncertainties applicable to the DNB LCO

ASI_{DNB} - Axial shape index associated with P_{fdn}.

*Equations 3-2 and 3-3 are valid for the excore and incore monitoring systems, respectively

Temperature, pressure and flow components of the DNB LCO are represented by equations as follows:

[redacted] (3-4)

(3-5)

(3-6)

where

P^{DNB}, $\dot{}^{DNB}$, T_{in}^{DNB} = Coolant conditions used in the calculations of (P_{fdn}, I_p) ordered pairs of data.

3.1.2 LHR LCO

The excore detector monitored LCO on linear heat rate is represented by the ordered pairs (P_{fdl}, I_p). A lower bound is drawn under the "flyspeck" data such that all the core power distributions analyzed are bounded. This lower bound is reduced by the applicable uncertainties and allowances to generate the LCO as follows:

[redacted] (3-7)

(3-8)

where:

B_{LHR}^{LCO} - Linear Heat Rate Power Limit for LCO after inclusion of uncertainties.

P_{fdl}^{LCO} = the power to the LCO linear heat rate limit including the effects of azimuthal tilting.

SMLO - Statistically combined uncertainty applied to the LHR LCO.

The incore detector monitored LCO on linear heat rate will not be modified for a statistical combination of uncertainties.

3.2 IMPACT OF STATISTICAL COMBINATION OF UNCERTAINTIES

3.2.1 IMPACT ON MARGIN

The motivation for using a statistical combination of uncertainties is to improve NSSS performance through a reduction in analytical conservatism in the uncertainties which must be taken into account. This section contains a discussion of the margin obtainable through a reduction in this conservatism.

Table 3-2 lists the uncertainty values previously used on Calvert Cliffs Units 1 and 2. The approximate worth of each of these uncertainties in terms of percent overpower margin (P_{fdn}, P_{fdl}) is shown.

The total uncertainties previously applied to the excore monitored DNB and LHR LCO are approximately [ ], respectively. The use of the statistical combination of uncertainties justifies a reduction in the conservatism in the uncertainty of approximately [ ], respectively. The use of the statistical combination of uncertainties and incore detector monitoring of the DNB LCO results in an uncertainty of approximately [ ].

Although the conservatism in the uncertainty has been reduced, a high degree of assurance remains that acceptable limits will not be exceeded.

3.2.2 IMPACT ON CONSEQUENCES OF DBE'S

The plant technical specifications restrict operation to within the DNB, LHR and equipment LCO's. The statistical combination of uncertainties only impacts the DNB and LHR LCO's. For transient analyses of DBE's where changes in DNB and LHR are significant, the appropriate LCO establishes the limits on initial conditions assumed in the analyses. Thus, the impact of uncertainties on these limits and, consequently, on the initial conditions for the transients, must be evaluated.

As explained in previous sections the LCO's are generated based on the P_{fdn} (for DNB), P_{fdl}^{LCO} (for LHR) and the ROPM for the limiting AOO. As explained in Appendix C, the maximum ROPM which bounds the maximum variations in the ROPM due to the range of uncertainties is used to generate these LCO's. Since the uncertainties will be combined statistically, the conservatism

in the uncertainties used to generate the LCO's are reduced.However, the DNB and LHR LCO's based on the methodology presented in this report will provide at least a 95% probability at a 95% confidence level that acceptable limits will not be exceeded during DBE's initiated from the extremes of the LCO's.

TABLE 3-1

UNCERTAINTIES ASSOCIATED WITH THE DNB AND LHR LCO'S

Uncertainty*	LHR LCO	DNB LCO
Core power (% of rated power)	± 2%	± 2%
Primary coolant mass flow (% Design flow)	NA	[ ]
Primary coolant pressure (psia)	NA	± 22
Core coolant inlet temperature (°F)	NA	± 2.
Power distribution (peaking factor)	7%	6%
Axial Shape Index (Excore Detector System)*		
1. Separability (asiu)	See Table A-1 of Appendix A1	
2. Calibration (asiu)	[ ]	[ ]
3. Shape Annealing (asiu)	[ ]	[ ]
4. Monitoring system processing (asiu)(2σ)	[ ]	
5. Monitoring system processing (psia)(2σ)		[ ]
Axial Shape Index (Incore Detector System) (ASIU)		[ ]

*Note: For complete description of these uncertainties, see Appendix A.

TABLE 3-2

IMPACT OF STATISTICAL COMBINATION OF

UNCERTAINTIES ON MARGIN TO LIMITS

FOR EXCORE MONITORING

Uncertainty	Previous Value	Approximate Values of Equivalent Overpower Margin DNB LCO	LHR LCO
Power	2% of rated	[	]
Core coolant inlet temperature	2 °F		
Reactor coolant system pressure	22 psi		
Axial shape index:			
Separability	[ ]		
Shape Annealing	[ ]		
Calibration	[ ]		
Reactor coolant system flow	[ ]		
Peaking factors	6% DNB, 7% LHR		
Equipment processing:			
DNB LCO	[ ]		
LHR LCO	[ ]		
	TOTAL		
Less previously approved NRC credit for statistics			
Total Uncertainty Applied Previously			
Total Uncertainty Statistically Combined (Excore)			
Net Margin Gain (Excore)			]

APPENDIX A

Basis for Uncertainties Used in Statistical Combination of Uncertainties

A.1 Shape Index Uncertainties

Two sets of instruments supply information for the calculation of axial shape index to assure that the Technical Specifications Limiting Conditions of Operation on DNB are met. One of these instrument systems is that set of excore detectors designated as "control channels". The other is the set of incore detectors. Each set of instruments is used for the Calvert Cliffs Units 1 and 2 Nuclear Steam Supply Systems in different monitoring systems.

A.1.1 Axial Shape Index Uncertainties Associated with the Excore Detector System

The control channel excore detectors are used in the power ratio recorder monitoring system for the Calvert Cliffs Units. They have geometric placement similar to that of the safety channel excore detectors used for the limiting safety system settings. These instruments are located at the same radial distance from the center of the core and at the same angular displacement from the main diameter of the core as the safety channel instruments, but on the opposite side of the diameter. Hence, the shape index[ ]uncertainty components described in Appendix A of Part 1 of this report (Reference A-1) not including those[ ]uncertainties due to instrument and calculator circuitry, are appropriate for the stochastic simulation of LCO uncertainties. These values are given in Table A -1.

The circuits used in monitoring the axial shape index with the control channel excore detector instruments for the DNB LCO are not the same as those for the TM/LP or linear heat rate LSSSs. The components of the LCO circuits may therefore introduce a different uncertainty into the stochastic simulation process. A root-sum square evaluation of the shape index uncertainty due to the Calvert Cliffs Units' LCO circuits results in the 95% probability, 95% confidence level estimated uncertainties listed in Table A -1. These values are appropriate for the stochastic evaluation of the net LCO uncertainties.

A.1.2 Axial Shape Index Uncertainties Associated with the Incore Detector System

The incore detectors are used to calculate the core average axial shape index, $\overline{I}$. The value of $\overline{I}$ calculated from the incore signals is used to monitor the DNB LCO in the BASS system. The methods used in this calculation are described in Reference A-2.

There are several uncertainties involved in the calculation of $\overline{I}$. They are identified in Table A-2, and are briefly described below.

1. [redacted]

2. [redacted]

3. [redacted]

4. [redacted]

5. [redacted]

6. [redacted]

7. [ ]

At least 95/95 confidence/probability values of each of these uncertainties are displayed in Table A1-2.

A.2 Measurement Uncertainties

The description of the measurement uncertainties given in Appendix A2 of Part 1 is also valid for the DNB LCO uncertainty evaluation.

A.3 Monitoring System Processing Uncertainties

A.3.1 Excore Monitoring System

The description of the Trip System Processing Uncertainties given in Appendix A3 of Part 1 is valid for the Calvert Cliffs excore monitored DNB LCO because that description is also based on excore detector input. The specific uncertainty components which reflect the differences in circuitry between the Safety and Control Channel processors is explicitly accounted for in the evaluation of the instrument processing uncertainty and the stochastic simulation procedure. The processing uncertainty on I_p is given in Table A -1.

A.3.2 In-Core Monitoring System

The processing uncertainties for the DNB LCO in-core monitoring system result from the [

]

A.4 References for Appendix A

A-1 CEN-124(B)-P "Statistical Combination of Uncertainties Part 1," December 1979

A-2 CEN-119(B)-P, "BASSS: Use of the In-core Detector System to Monitor the DNB-LCO on Calvert Cliffs Unit 1 and Unit 2", November 1979

A-3 "INCA, Method of Analyzing In-core Detector Data in Power Reactors," CENPD-145-P, April 1975

A-4 Letter, R. W. Reid (NRC) to A. E. Lundvall (BG&E) "Safety Evaluation Report for Calvert Cliffs Unit 1 Cycle 4," June 14, 1979

TABLE A -1

Uncertainty [and Bias] Components for the Evaluation of the LCO Related Peripheral Shape Index(1)

	$K\sigma$ 95/95 ASIU	K(f)(2)	[ ]
1. Separability Uncertainty			
2. Calibration uncertainty(n)			
3. Shape annealing uncertainty(n)			
4. Processing uncertainty(n)			
LHR (ASIU)			
DNB (PSIA)			

Notes on Table A1-1:

(1) All components of the peripheral shape index have been tested for normality [ ]

(2) f - degrees of freedom

(3) [ ]

(4) [ ]

(5) 2 Sigma values for consistent sets of input to the uncertainty processors

Table A-2

Uncertainties Associated with the Evaluation of the Core Average Axial Shape Index, $\overline{I}$, Using the Incore Detector System

	Parameter	>95/95 Value of Uncertainty, ASIU
1.		
2.		
3.		
4.		

APPENDIX B

Summary of Previous Methods for Combining Uncertainties

The methods previously used for the application of uncertainties to the LCO's are presented in Reference B-1 and are summarized in this appendix.

B.1 LHR LCO

The LCO limit on linear heat rate is represented by the ordered pairs (P_{fdl}, I_p). A lower bound is drawn under this "flyspeck" data such that all the core power distributions analyzed are bounded. Using the previous methodology this lower bound was reduced by the applicable uncertainties and allowances to generate the LHR LCO as follows:

[ ] (B-1)

(B-2)

where:

[ ] (B-3)

W^{LCO}_{max} = LCO limit on linear heat rate

W_{avg} = Core average linear heat rate

F_{xy} = Planar radial peaking factor

F_z = Core average axial power distribution peaking factor

F_{aug} = Fuel densification-dependent power peaking augmentation factor

T_{AZ} = Azimuthal tilt allowance

PU = Uncertainty in predicting local power at the fuel design limit

BMU = Power measurement uncertainty

SAU = Shape annealing factor uncertainty

RSU = Shape index separability uncertainty

ACU = Axial shape index calibration uncertainty

APU = Processing uncertainty

B.2 DNB LCO

The fuel design limit for the DNB LCO is represented by the ordered pairs (P_{fdn}, I_p). A lower bound is drawn under the "flyspeck" data such that all the analyzed core power distributions are bounded. Using the previous methodology this lower bound was reduced by applicable uncertainties and allowances to obtain ex-core monitoring limits as follows:

[ ] (B-4)

(B-5)

where:

P'_{fdn} - Power to fuel design limit on DNB

SC - approved partial credit for conservatism in uncertainty application

BMU - Power measurement uncertainty

Other components of the DNB LCO were then represented by equations as follows:(21-1)

[ ] (B-6)

(B-7)

(B-8)

PMU - Pressure measurement uncertainty

TMU - Temperature measurement uncertainty

FMU - Flow measurement uncertainty

B.3 References for Appendix B

B -1 CENPD-199-P, "C-E Setpoint Methodology," April, 1976.

APPENDIX C

TREATMENT OF UNCERTAINTIES IN TRANSIENT ANALYSES

APPENDIX C

TRANSIENT ANALYSIS

C.1 Objective of Analysis

As stated in Section 3.1, the DNB and LHR LCO's are generated from the following:

1. The P_{fdn} (for DNB) and P_{fdl}^{LCO} (for LHR) for the reload core.
2. Statistically combined process variable uncertainties.
3. The DNB and LHR Required Overpower Margin (ROPM) for the limiting AOO.

The methods used to combine uncertainties were discussed previously. The objectives of this appendix are:

1. To evaluate the impact of statistically combining uncertainties on the selection of initial conditions used in the transient analysis of DBE's.
2. To determine the magnitude of the variation in ROPM attributable to the uncertainties.

C.2 General Strategy

This section of the appendix provides the basis for analyzing the Loss of Coolant Flow (4 Pump LOF) and Single Full Length CEA drop (CEA drop) events to determine the variation of the ROPM due to statistically combining uncertainties.

The Design Basis Events (DBEs) applicable to Calvert Cliffs Unit 1 and Unit 2 are presented in Table C-1. This table also lists the RPS trips which intervene to assure that acceptable limits* are not exceeded. The table also identifies which of these events has the potential of yielding the maximum ROPM used to generate DNB or LHR LCO's, or for setting the pressure bias input used to establish the TM/LP LSSS.

---

* The term "acceptable limits" is used in this appendix to include limits on DNBR, kw/ft, and dose rates, etc.

This table shows that most of these events can be classified in the following manner:

1. The events where action of the Thermal Margin/Low Pressure (TM/LP) trip and/or the Local Power Density (LPD) trip is necessary to prevent exceeding acceptable limits.

2. The events where action of RPS trips and/or sufficient initial steady state margin is necessary to prevent exceeding acceptable limits.

These two categories of events are further discussed below.

C.2.1. Events Where Action of TM/LP and LPD Trips is Necessary to Prevent Exceeding Acceptable Limits

The TM/LP trip limits are calculated assuming a conservative pressure bias factor. This bias factor accounts for the margin degradation due to processing, equipment and RTD response time delays. By accounting for these effects in a conservative manner, the TM/LP trip will be actuated when necessary to ensure that the DNBR limit is not exceeded.

As stated in Reference C-1, the maximum pressure bias factor is obtained either for the RCS Depressurization event or the CEA Withdrawal (CEAW) event. However, the CEAW event now has been classified (in Reference C-2) as not requiring the TM/LP trip. Thus, this event is no longer analyzed to determine the pressure bias factor. It is analyzed to determine ROPM as described in Reference C-2. The pressure bias factor calculated for the RCS Depressurization event (which is the most rapid depressurization event where mitigation by the TM/LP trip is necessary) is used to generate the TM/LP trip limits.

The pressure bias term for the RCS Depressurization event, calculated using the methods and procedures given in Reference C-1, is the maximum pressure bias term for the entire operating range of system parameters allowed by the Technical Specification LCO. Since the methods and the initial conditions used in this analysis are selected in the same manner as described in Reference C-1, there is no need to perform a

sensitivity study on the calculated value of the pressure bias term. That is, the method of combining uncertainties (either statistical or deterministic) does not affect the way in which the TM/LP trip is used for protection for DBE's where actuation of the TM/LP trip is required.

The events listed in Table C-1 where action of the LPD trip is necessary to prevent the kw/ft limit from being exceeded do not provide any bias term for input to the LPD trip limits. These limits already include a three percent power bias to account for any transient variations in the measured power. Since none of the DBE's requiring the LPD trip result in a three percent margin degradation from the time of LPD trip signal to the time of maximum kw/ft, there is no need to input an additional bias for the LPD trip based on transient analysis. Therefore, the method of combining uncertainties has no impact on the method of analysis or the input data selected for transients requiring the actuation of the LPD trip to ensure kw/ft SAFDL limit is not exceeded.

C.2.2 Events for Which Intervention of RPS Trips and/or Sufficient Initial Steady State Thermal Margin Maintained by LCO is Necessary to Prevent Exceeding Acceptable Limits.

DBE's listed in this category are not solely protected by the TM/LP and LPD trips because some of the parameters (such as core mass flow rate or radial peaking factors) that are important in some DBE's are not directly monitored by the TM/LP and LPD trips. For these DBE's, the mitigating effects of RPS trips and/or sufficient initial steady state margin maintained by operating within the LCO is necessary to ensure that acceptable limits are not exceeded.

The DBE's in this category can be further grouped according to a single key parameter change which has the greatest impact on the margin degradation. A grouping of DBE's in this manner is presented in Table C-2.

To determine the sensitivity of ROPM to the magnitude of uncertainties listed in Table C-3 during an event characterized mainly by a decrease in the core mass flow rate, the 4 Pump LOF event was analyzed. This event was analyzed because it can provide limiting input (i.e., ROPM) to establish the DNB LCO. The variation of ROPM due to the magnitude of uncertainties observed for the 4 Pump LOF event bounds that for all events characterized by decreases in the core mass flow rate, since all of these events are characterized by the same principal physical effects.

The CEA drop event was analyzed to determine the variation of ROPM due to the method of calculating uncertainties for events characterized by increases in integrated radial and planar peaking factors (F_r, F_{xy}). This event was analyzed because a dropped CEA results in higher F_r and F_{xy} increases than the Asymmetric Steam Generator events. Thus, the ROPM for the CEA drop is higher than for the Asymmetric Steam Generator event and can provide limiting input for establishing the LCO.

The CEA Withdrawal event was not analyzed because the ROPM for this event is approximately two percent lower than the CEA drop event. In addition (based on the results showing insensitivity of ROPM to the magnitude of uncertainties for the 4 Pump LOF and CEA drop events) it can be stated that this event will not become limiting from the standpoint of establishing LCO's due to variations in the ROPM attributable to the process variable uncertainties considered in the analyses.

C.2.3 Impact of Statistically Combining Uncertainties on DBEs with Other Limits

The statistical combination of uncertainties are only used to establish DNB and LHR LCO's and LSSS. Therefore, it impacts only the DNB- and LHR-related LCO's and LSSS. Statistically combining uncertainties does not impact events with other limits (such as deposited energy, time to lose Technical Specification allowed shutdown margin, etc.). Therefore, events with other limits will be analyzed using the same methods and selecting the initial conditions in the same way as previously reported in the FSAR (Reference C-3) or as updated by approved reload license amendments.

C.2.4 Impact of DNB Monitoring Systems (In-core vs. Ex-core) on ROPM

As stated in Section 1.2.1, the DNB LCO can be monitored using either the ex-core detectors or the in-core detectors. The basic difference in uncertainties between these two monitoring systems are the values of the[ ]uncertainties. The ROPM is calculated parametric in axial shape index. The uncertainty associated with any given value of[ ]is accounted for in the analyses which determines the LCO. Hence, there is no impact from the different[ ](using ex-core or in-core detectors) on the calculated ROPM.

C.3 Analyses Performed for Evaluation of ROPM for the Limiting DBEs

C.3.1 Loss of Coolant Flow Event (4 Pump LOF)

C.3.1.1 Description of Transient

The key input parameters for the 4 pump LOF event are determined from the description of the transient given below.

The 4 pump LOF event is assumed to be initiated by the simultaneous loss of AC power to all four reactor coolant pumps. After the loss of power, the flow starts coasting down rapidly. In a very short time (about 1.0 second) the low flow trip setpoint is reached. After a delay for processing the trip signal (~0.5 second) and decay of the magnetic flux for the holding coils (~0.5 second), the CEAs start dropping into the core. After the scram rods reach about 20% insertion for an initially top peaked axial shape (or 55% insertion for a bottom peaked shape), the CEAs have inserted sufficient negative reactivity to drop the core heat flux below that required to turn around the transient DNBR. The transient minimum DNBR occurs when the rate of heat flux decay (after scram) equals the rate of flow decrease. The minimum DNBR occurs within 3.0 to 4.0 seconds of the initiation of this event.

Since the minimum DNBR is reached within the first 4.0 seconds, the power distributions and the peak linear heat generation rate have not had time to change. The core inlet and fuel temperatures will not change appreciably, since the loop cycle time (~10.0 seconds) and the fuel time constant (~6.0 seconds) are larger than the time required to terminate the transient DNBR. Thus, the margin degradation for this event is determined primarily by:

1. The core flow coastdown
2. The signal processing time delay
3. The holding coil time delay
4. The low flow trip setpoint
5. The available scram worth
6. The CEA reactivity versus insertion characteristics.

C.3.1.2 Criteria of Analysis

This event is classified as an AOO and hence is analyzed relative to the

following criteria:

1. Minimum Transient DNBR $\geq$ DNBR limit based on CE-1[1] correlation.
2. Centerline Temperature Melt[2] $\leq 5080^{0}F - \frac{280 \times \text{Burnup (MWD/MT)}}{50{,}000 \text{ (MWD/MT)}}$

Notes: 1) CE-1 DNBR shall have a minimum allowable limit corresponding to a 95% probability at a 95% confidence level that DNB will not occur on the limiting rod. In this study, a DNBR limit of 1.23 was used (See Ref. C-4 for justification.)

2) The CTM SAFDL is a criterion for this event, but this SAFDL is never exceeded since there is no increase in PLHGR during this event.

C.3.1.3 Input Parameters and Initial Conditions

The purpose of this study is to evaluate how much predicted margin degradations vary because of the way the uncertainties of initial conditions are combined. An analysis parametric in

1. the initial coolant temperature
2. initial RCS pressure
3. initial core mass flow rate
4. initial axial shape index
5. integrated radial peaking factor, and
6. initial core power

was performed to determine the sensitivity of ROPM to these parameters. Other parameters were assumed to be at their limiting values to maximize the calculated margin degradation. The input parameters used in the analysis of the 4 Pump LOF event are presented in Table C-4. A brief justification of values selected is given below.

The key parameters for the loss of coolant flow event were identified earlier as the flow coastdown, the RPS delay times, the low flow analysis trip setpoint and the scram reactivity versus insertion characteristics.

The flow coastdown assumed in the analysis is presented in Figure C-1. The coastdown was calculated assuming that the coastdown assist feature is inoperative. This produces the most rapid coastdown, and thus the maximum margin degradation due to the lower absolute flow at time of minimum DNBR.

The low flow analysis trip setpoint of 93% assumed is one corresponding to the minimum allowed Technical Specification limit for initial 4-pump flow. The RPS trip processing response delay time and holding coil magnetic flux decay time assumed in the analysis are the maximum values allowed by the Technical Specifications. The use of maximum delay times results in the largest margin degradation since it takes longer for the CEAs to start dropping into the core and thus takes a longer time period to turn around the transient DNBR. The scram reactivity versus insertion characteristics assumed in the analysis were calculated according to the methods given in Reference C-5.

Other important parameters are the available scram worth and the moderator and fuel temperature reactivity coefficients (MTC and FTC). The available scram worths were conservatively calculated, including an allowance for the most reactive CEA being stuck in the fully withdrawn position after the trip.

A beginning-of-life (BOL) MTC was used in the analysis, since a positive MTC in combination with the slight increase in the coolant temperatures accelerates the rate of increase of both the coolant temperature and heat flux prior to trip. Both these effects cause the transient DNBR to decrease at a faster rate. A BOL FTC is assumed for the same reasons.

C.3.1.4 Method of Analysis for the Four Pump LOF

The Nuclear Steam Supply System (NSSS) response to a 4 pump LOF event was simulated using the digital computer code CESEC described in Reference C-6. The code STRIKIN (Ref. C-7) was used to calculate the time variation in core average and hot channel heat flux during the 4 pump LOF event. The thermal hydraulic code TORC (Ref. C-8) incorporating a CE-1 correlation and a 1.23 DNBR limit was used to calculate the thermal margin degradation during the event. The COAST code, described in Reference C-9, was used to calculate the flow coastdown during this event. These codes and methods are the same as described in previously approved license submittals (Ref. C-10) except for the use of a DNBR limit of 1.23 rather than the 1.19 value used previously.

The calculational procedures used in the analysis to determine the DNB ROPM depend upon the initial axial power distribution. The methods used to analyze 4 pump LOF are axial shape index dependent because credit for the heat flux decay is taken only when the initial minimum CE-1 DNBR is located in an axial region of the core where the scram rods have passed the axial node of minimum DNBR before the time of minimum DNBR is reached.

For axial power distributions characterized by negative shape indices, the STRIKIN-TORC method was used. This method is schematically presented in Figure C-2. For axial power distribution characterized by positive shape indices, the CESEC-TORC method, presented in Figure C-3. was used. For a zero shape index both methods are used to calculate the ROPM and the maximum value obtained by these methods is then used to generate LCO's.

The two methods used to analyze this event are discussed below.

C.3.1.4.1. STRIKIN-TORC Method

1. The time-dependent core flow, the individual loop flows and steam generator pressure drops are determined by using the code COAST. COAST solves the conservation equations for mass flow and momentum. The general forcing functions for the fluid momentum equations consist of the pump torque values from the manufacturer's four quadrant curves, wherein the torque is related to the pump angular velocity and discharge rate.

2. Limiting axial power distributions, characterized by shape index, are determined from a large sample (~2,000) of possible distributions which are calculated as a function of axial shape index, core burnup, and CEA configuration, using the QUIX code (Reference C-11). The limiting axial power shapes are those distributions that produce the lowest initial steady state power to a DNBR limit of 1.23 at a given axial shape index. The power at which the limit is reached is predicted by the TORC code.

It should be noted that steps 1 and 2 are independent of the LOF method, (i.e., STRIKIN-TORC or CESEC-TORC) used.

3. The resultant core flows are used as input to CESEC to determine the hot channel mass flow rate and to demonstrate that Reactor Coolant System (RCS) pressure during the transient does not exceed the pressure limit of 2750 psia (110% of design).

4. The RCS flow coastdown, the hot channel flow coastdown from CESEC, axial power distributions, and corresponding scram curves are input into STRIKIN-II to determine the time dependent hot channel and core average heat flux distributions during the transient. The use of STRIKIN-II to calculate the absolute core average and hot channel heat flux distributions as a function of time is consistent with the methodology utilized and

approved by the NRC on Calvert Cliffs Unit 1 Cycle 2 (Reference C-10) and Millstone Point Unit 2,Cycle 3 (Reference C-12).

5. The TORC code is used to determine the time of minimum DNBR. The inputs to the code are the core mass flow rate as well as the hot channel and core average heat fluxes predicted by STRIKIN-II at times of interest. Other parameters input to TORC are the initial RCS pressure, the initial inlet temperature, the initial integrated radial peaking factor and the net uncertainties combined statistically.

6. The core mass flow rate and the hot channel and core average heat flux profile at the time of minimum DNBR are used in conjunction with the initial values of inlet temperature, integrated radial peaking factor, RCS pressure and the net uncertainties combined statistically to obtain a power at which the fuel design limit on DNBR is reached for the transient conditions. The power at the time of minimum DNBR is denoted B_2.

7. A TORC case is also run to determine the rod average power at which the fuel design limit on DNBR is reached for the initial steady state system parameters. This value of power is designated B_1.

8. The FOPM is then defined (Ref.C-1) to be:

$$[\qquad\qquad] \qquad (C\text{-}1)$$

C.3.1.4.2 CESEC-TORC Method

1. Steps 1 and 2 outlined for the STRIKIN-TORC method are also used for this method to obtain the flow coastdown data and the limiting axial power distributions.

2. The core coolant flow, as a function of time, along with axial power distribution, initial coolant inlet temperature, initial RCS pressure and the scram reactivity versus insertion associated with the axial power distribution of interest are input to CESEC to obtain the time dependent values of core average heat flux, RCS pressure, coolant inlet temperature and the core mass flow rate.

3. A set of TORC cases are run with the time dependent values of core heat flux, temperature, RCS pressure and core mass velocity along with the initial values of integrated radial peaking factor, the axial power distribution and the net uncertainties combined statistically to determine the time of minimum DNBR.
4. The core mass velocity at the time of minimum DNBR in combination with the initial values of RCS pressure, inlet temperature, axial power distribution, integrated radial peaking factor, core average heat flux and the net uncertainties combined statistically are used to determine the power to the DNB limit. This power is denoted B_2.

5. A TORC case is also run with the initial steady state system parameters, including statistically combined uncertainties, to determine the power to DNB limit. This power is denoted B_1.

6. The ROPM is then, as before, defined to be

$$[\qquad\qquad] \qquad (C-2)$$

C.3.1.5 Results

The results of the sensitivity analysis performed over the range of uncertainties for the variables listed in Table C-3 about the nominal base conditions listed in Table C-4 are presented in Figure C-4. This figure presents the ROPM as a function of initial axial shape index obtained for the event initiated from the nominal base conditions and also presents the maximum variation in the ROPM due to the uncertainties. It should be noted that the absolute value of the ROPM is plant and cycle specific; however, the maximum margin variation is not plant and cycle specific. The maximum variation in the ROPM, shown in Figure C-4 as a function of axial shape index, will be added to the cycle specific ROPM calculated for the nominal base conditions to obtain the maximum ROPM during the event. This maximum ROPM will be used to establish the DNB LCO.

The sequence of events during a 4 pump LOF event is presented in Table C-5. The NSSS response during this event is presented in Figures C -5 to C-8.

C.3.1.6 Conservatisms in the Analysis Methods.

The purpose of this section is to identify the conservatisms that are included in the methods used to calculate the ROPM on DNBR during a 4 pump LOF event.

1. The magnetic flux decay of the holding coil assumed in the analysis is 0.5 second. A more realistic value based on field test data is 0.4 second.

2. The low flow response time assumed in the analysis is 0.50 second, which is conservative by at least 0.1 second based on field measurements.

3. The CEA drop time to 90% insertion value of 3.1 seconds assumed in the analysis is for slowest CEA. A more realistic value for the slowest CEA drop time to 90% insertion is 2.90 seconds.

4. The flow coastdown assumed in the analysis does not take credit for the coastdown assist feature. A more realistic flow coastdown presented in Figure C -9, would be slower than assumed in the analysis.

5. The ROPM is calculated without taking credit for the higher value of RCS pressure at the time of minimum DNBR. The higher RCS pressure at the time of minimum DNBR will lower the ROPM for this event.

To quantify the conservatisms outlined above a "best estimate" case was run. A comparison of the input data used in the safety analysis case described in Section 2.3 with that used in the best estimate case is presented in Table C -6.

The ROPM for the best estimate case is [ ], which is lower by [ ] than that for the transient analysis case. The results of the best estimate case show that due to the slower flow coastdown and the higher low flow trip setpoint assumed in the best estimate case, the low flow trip is initiated at the same time as in the safety analysis case. However, the faster RPS response time, the faster time to decay the magnetic flux of the holding coil and the faster insertion of the shutdown CEAs turns around the transient DNBR faster relative to the safety analysis case. Due to the slower flow coastdown, the absolute flow at the time of

minimum DNBR is higher than in the transient analysis case.

The sequence of events for the best estimate case is given in Table C-7. The NSSS response for the best estimate is given in Figures C-10 to C-13.

C.3.2 Single Full Length CEA Drop Event (CEA Drop)

C.3.2.1 Description of Transient

The key input parameters for the CEA Drop event are determined from the description of the transient given below.

A CEA Drop event is assumed to occur as a result of:

1. An inadvertant interruption of power to the CEA holding coil, or
2. A failure in the latching mechanism when CEAs are being moved.

The drop of a CEA into the core reduces the fission power in the vicinity of the dropped CEA and adds negative reactivity on a core-wide basis. The negative reactivity causes a prompt drop in power and thus the heat flux. The magnitude of this prompt power decrease depends upon the worth of the dropped CEA. Since no credit is taken for turbine runback in the analysis, a power mismatch exists between the primary and secondary system. The power mismatch initially causes the primary side to cool down. The decrease in the fuel and moderator temperatures in conjunction with an assumed highly negative fuel temperature and moderator temperature coefficients adds positive reactivity. The positive reactivity added by the feedbacks compensates for the negative reactivity added by the dropped CEA within approximately 100 seconds.

The initial decrease in the coolant temperatures also causes the pressurizer pressure to decrease (the analysis conservatively assumes that the pressurizer level and pressure control systems are inoperative). In addition, the dropped CEA also causes an asymmetry in the radial power distribution and the radial power peaks. The radial peaks increase as a result of this distortion and achieve a new, "tilted" asymptotic state. At approximately 100 seconds, the power and the core heat flux have returned to their initial values. The coolant inlet temperature and RCS pressure achieve a new, lower, steady state value. The DNBR also achieves a new, lower, steady state value.

The margin degradation during this event is a result of the following changes in the key variables described above, which are:

1. Increase in radial peaking factors.
2. Decrease in RCS inlet coolant temperature.
3. Decrease in RCS pressure.

C.3.2.2 Criteria of Analysis

The criteria of analysis for this event are the same as for the 4-pump LOF event. However, in this event the peak linear heat rate increases. Therefore, the CTM criterion must also be addressed.

C.3.2.3 Input Parameters and Initial Conditions

This study evaluates how the uncertainties are applied to select initial conditions for the transient analyses in the CEA drop event. An analysis parametric in

1. the initial inlet temperature,
2. initial RCS pressure,
3. initial RCS flow,
4. initial axial power distribution,
5. integrated radial peaking factor, and
6. initial core power

was performed to determine the sensitivity of ROPM to these parameters. Other parameters were assumed to be at their limiting values to maximize the calculated margin degradation. The method used for this analysis is schematically presented in Figure C-14. The input parameters used in the analysis of the CEA drop event are presented in Table C-8. For completeness, a brief justification of each parameter assumed in the analysis is given below.

The reactor state parameters of primary importance in determining the margin degradation are: (1) the integrated radial peaking factor for DNBR ROPM, (2) the planar radial peaking factor for LHR ROPM, and (3) the CEA drop worth. The analysis conservatively assumed the maximum integrated and planar radial peak changes and the minimum CEA drop worth. The maximum radial peaking factor change results in the highest ROPM. Assuming a minimum CEA drop worth is also conservative since it minimizes both the pressure and inlet temperature decreases. (It should be noted that the analysis assumes an inconsistent set of radial peaking factor changes and CEA drop worth. Realistically, a low reactivity worth dropped CEA will not produce the maximum radial peaking factor increases.)

End of life values of Moderator Temperature Coefficient (MTC) and the Fuel Temperature Coefficient (FTC) were assumed in the analysis. These negative FTC and MTC in conjunction with the decreasing coolant and fuel temperatures insert positive reactivity. The positive reactivity inserted offsets the negative reactivity inserted initially by the dropped CEA and thus enables the core power to return to its initial value. The uncertainties on the FTC assumed are given in Table C-8. All control systems are assumed to be in the manual mode. The key control systems for this event are the Pressurizer Pressure Control System (PPCS) and Pressurizer Level Control System (PLCS). The PPCS and PLCS are assumed to be in the manual mode because this allows the primary pressure to drop during the transient and thus minimizes the pressure at time of minimum DNBR. This results in the largest DNBR margin degradation during the event.

C.3.2.4 Method of Analysis for the CEA Drop Event.

The Nuclear Steam Supply System (NSSS) response to a single full length CEA drop event was simulated using the digital computer code CESEC, described in Reference C-6. The thermal hydraulic design code TORC, described in Reference C-8, used the CE-1 correlation and a DNBR limit of 1.23 to calculate the thermal margin degradation during the transient.

C.3.2.5 Required Overpower Margin for CEA Drop.

C.3.2.5.1 Required Overpower Margin on DNBR.

The calculation procedures used in the analysis to determine DNB ROPM are presented in Figure C-14. This procedure consists of the following steps:

1. Determining the pseudo hot channel power distribution both before CEA drop and after CEA drop. The integrated radial peaking factors are synthesized from the core average axial power distribution and planar radial power distributions.

2. Simulating the CEA drop event using CESEC to determine the final values of core average heat flux, RCS pressures and inlet temperature.

3. Running the TORC code to determine the rod average power at which the final design limit on DNBR is reached for the initial steady state parameters including uncertainties combined statistically. This value of power is denoted B_1.

4. The maximum heat flux, final inlet temperature and RCS pressure, the post drop integrated radial peaking factor, the post drop axial power distribution, the uncertainties combined statistically and the final value of the core average mass velocity are input to TORC to determine the power at which the fuel design limit on DNBR is reached for the transient conditions. This power is denoted B_2.

5. The ROPM is then defined as:

$$[\qquad\qquad\qquad\qquad\qquad\qquad\qquad\qquad\qquad\qquad\qquad\qquad] \qquad \text{(C-3)}$$

where P_1 is the initial power level and P_2 is the final power level of the core.

C.3.2.5.2 Required Overpower Margin on PLHGR (KW/FT).

The ROPM on linear heat rate is calculated by the procedures given in Chapter 8 of Reference C- 1. Since the methods used to analyze the PLHGR have not changed and since there is no sensitivity of the ROPM due to statistically combining uncertainties, no analysis is required.

C.3.2.6 Results.

The results of the sensitivity analyses performed for the CEA drop event is presented in FigureC -13. This figure presents the ROPM as a function of initial axial shape index obtained for the event initiated from the nominal base conditions and also presents the maximum variation in the ROPM due to the uncertainties. The maximum variation in the ROPM, shown in Figure C-15 as a function of axial shape index, will be added to the cycle specific ROPM calculated for the nominal base conditions to obtain the maximum ROPM during the event. This maximum ROPM will be input to establish the DNB LCO.

The sequence of events during a CEA drop event is presented in Table C -9. The NSSS response during this event is presented in Figures C-16 toC -19.

C.3.2.7 Conservatism in Analytical Methods.

The purpose of this section is to identify the conservatisms that are included in the methods used to calculate the ROPM on DNBR during a CEA drop event. These conservatisms are qualitatively identified below. An example case is presented and compared with the safety analysis results of previous sections to quantify the conservatism.

1. The analysis assumed a bounding value for the integrated radial peaking factor changes which is conservative by 2%. The analysis also assumed a minimum CEA drop worth, which does not produce the maximum integrated radial peaking factor changes. The use of consistent set of CEA drop worth and the integrated radial peaking factor change will lower the margin degradation.

2. No credit for the actuation of the pressurizer pressure and level control system is taken in the analysis. The actuation of the pressurizer pressure and level control system would maintain the RCS pressure at a higher value thereby lowering the margin requirement for this event.

3. The moderator temperature coefficient assumed in the analysis is the most negative value of $-2.5 \times 10^{-4} \Delta\rho/^{o}F$ allowed by the Technical Specifications. A more realistic end-of-life value, including measurement uncertainty, is $-2.3 \times 10^{-4} \Delta\rho/^{o}F$.

To quantify the conservatism outlined above a "best estimate" case was run. A comparison of the input data used in the transient analysis case described in Section C.3.2.6 with that used in the best estimate case is presented in Table C-10.

The ROPM for the best estimate case is [ ] which is conservative by [ ] with respect to the transient analysis case. The sequence of events for the best estimate case is presented in Table C-11 and the NSSS response during this event is given in Figures C-20 to -23.

C.4 CONCLUSIONS

Based on the results of the sensitivity studies, it can be concluded that:

1. The ROPM is relatively insensitive to the range of uncertainties on the initial conditions. The maximum ROPM established by the sensitivity study is used to generate the LCO's.

2. The use of a constant maximum ROPM at each axial shape index to generate the LCO's eliminates the need to stochastically simulate the ROPM variations in calculating the net aggregrate uncertainty.

3. The use of the maximum ROPM also ensures with a high degree of confidence that acceptable limits for the DBE's will not be exceeded.

C.5 REFERENCES FOR APPENDIX C

C-1 CENPD-199-P, "C-E Setpoint Methodology, April, 1976.

C-2 CEN-121 (B)-P, "Method of Analyzing Sequential Control Element Assembly Group Withdrawal Event for Analog Protected System", November, 1979.

C-3 Calvert Cliffs Unit 1 FSAR Docket No. 50-317.

C-4 CEN-124(B)-P, "Statistical Combination of Uncertainties Part 2 - Combination of System Parameters Uncertainties in Thermal Margin Analyses for Calvert Cliffs Units 1 and 2", January 1980.

C-5 CEN-122 (F), "FIESTA A One Dimensional, Two Group Space-Time Kinetics Code for Calculating PWR Scram Reactivities", November 1979.

C-6 CENPD-107, "CESEC TOPICAL REPORT", July, 1974.

C-7 CENPD-135 (P), "STRIKIN-II, A Cylindrical Geometry Fuel Rod Heat Transfer Program", August, 1974.

C-8 CENPD-161-P, "TORC Code, A Computer Code for Determining the Thermal Margin of a Reactor Core", July, 1975.

C-9 CENPD-98, "COAST Code Description", May, 1973.

C-10 Letter, D. L. Zieman (NRC) to A. E. Lundvall, Jr. (BG&E) dated March 14, 1977, License Amendment 21 and SER for Cycle 2 Operation of Calvert Cliffs Unit 1. Docket No. 50-317

C-11 System 80 PSAR, CESSAR, Vol. 1, Appendix 4A, Amendment No. 3, June, 1974.

C-12 Letter, R. W. Reid (NRC) to W. G. Counsil (NNEC) dated May 12, 1979, License Amendment 52 and SER for Cycle 3 Operation of Millstone Point Unit 2. Docket No. 50-336

TABLE C-1

DESIGN BASIS EVENTS AND RPS TRIP PROTECTION

DBE	RPS TRIP	LIMITING INPUT TO ESTABLISH SETPOINTS	
		LCO	LSSS
CEA Withdrawal	High Power and Variable High Power	No	No
Boron Dilution	TM/LP and/or LPD	No	No
Loss of Load	TM/LP and/or LPD	No	No
Excess Load	TM/LP and/or LPD	No	No
Loss of Feedwater	TM/LP and/or LPD	No	No
Excess Feedwater	TM/LP and/or LPD	No	No
RCS Depressurization	TM/LP and/or LPD	No	Yes
Loss of Coolant Flow	Low Flow	Yes	No
Loss of AC Power	Low Flow	No*	No
CEA Drop	None	Yes	No
Asymmetric Steam Generator Transients	ΔP Across Steam Generator (input to TM/LP)	No	No
CEA Ejection	High Power or Variable High Power	No	No
Seized Pump Rotor	Low Flow	No	No
Steam Line Rupture	Low Steam Generator Level or Low Steam Pressure	No	No
Steam Generator Tube Rupture	TM/LP and/or LPD	No	No

*The DNBR transient for this DBE is covered by the loss of coolant flow DBE transient analysis.

TABLE C-2

DESIGN BASIS EVENTS AND IMPORTANT PARAMETER CHANGES

Design Basis Event	Parameter Changes Most Important to Margin Degradation
Loss of Forced Primary Coolant Flow	Decrease in Core Mass Flow Rate
Loss of Non-Emergency AC	Decrease in Core Mass Flow Rate
Seized Rotor	Decrease in Core Mass Flow Rate
CEA Drop	Increase in Integrated Radial and Planar Peaking Factors
Asymmetric Steam Generator Transients	Increase in Integrated Radial and Planar Peaking Factor
CEA Withdrawal	Increases in Core Power and Core Coolant Inlet Temperature

TABLE C-3

UNCERTAINTIES

Uncertainties	Values
1. Uncertainty in integrated radial pin pow (F_r)	±6%
2. Uncertainty in local core power density (F_q)	±7%
3. Power measurement uncertainty	±2%
4. Shape Index uncertainty	**
5. Flow measurement uncertainty	±3%
6. Pressure measurement uncertainty	±22 psia
7. Temperature measurement uncertainty	±2°F

** ROPM is an input value used to generate the LCO's. The ROPM values are generated parametrically in axial shape index. The uncertainty associated with any given value of axial shape index is accounted for explicitly in the analyses which determine the LCO's and does not have to be accounted for in the transient analysis.

TABLE C-4

KEY INPUT PARAMETERS USED IN THE LOSS OF COOLANT FLOW EVENT

Parameter	Units	Values
Initial Power Level	% of 2710 MWt	100.0*
Initial Inlet Temperature	°F	548*
Initial Core Mass Velocity	$X10^6$ lbm/hr-ft^2	2.617*
Initial RCS Pressure	psia	2225*
Integrated Radial Peaking Factor -		
-ARO		1.65*
- Lead Bank Inserted		1.70*
Initial Axial Power Distributions		**
Low Flow Analysis Trip Setpoint	% of initial flow	93.0
Flow Coastdown	Fraction of Initial flow vs. time	See Figure C-1
Trip Delay Time	sec	050
Holding Coil Delay Time	sec	0.5
CEA Drop Time to 90% Insertion	sec	3.1
Moderator Temperature Coefficient	$X10^{-4}$ $\Delta\rho$/°F	+0.5
Fuel Temperature Coefficient Uncertainty	%	-15.0
CEA Scram Worth	%$\Delta\rho$	-5.3
Initial Axial Shape Index	asiu	-.2 to +.2

* Does not include uncertainty. The uncertainties for these parameters are given in Table C-3.

** The ROPM is calculated as a function of axial shape index characterized by various axial power distributions.

TABLE C -5

SEQUENCE OF EVENTS
LOSS OF COOLANT FLOW EVENT

Time	Event	Value
0.0	Loss of Power all Four Reactor Coolant Pumps	- -
1.0	Low Flow Trip	93% of initial flow
1.5	Trip Breakers Open	- -
2.0	CEAs Begin to drop into core	- -
4.9	Maximum RCS Pressure, psia	2280

TABLE C-6

COMPARISON OF KEY INPUT PARAMETER USED IN SAFETY ANALYSIS AND BEST ESTIMATE CASES FOR 4 PUMP LOF EVENT

Parameter	Units	Safety Analysis Case	Best Estimate Case
Initial Power Level	% of 2710 MWt	100.0	100.0
Initial Inlet Temperature	°F	548.0	548.0
Initial Core Mass Flow Rate	$X10^6$ lbm/hr-ft^2	2.617	2.617
Initial RCS Pressure	psia	2225	2225
Integrated Radial Peaking Factor (ARO)		1.65	1.55
Low Flow Analysis Trip Setpoint	% of initial flow	93.0	95.0
Flow Coastdown	Fraction of initial flow vs. time	Figure C-1	Figure C-9
RPS Time Delay	sec	0.50	0.40
Holding Coil Delay Time	sec	0.5	0.35
CEA Drop Time to 90% Insertion	sec	3.10	2.90
CEA Scram Worth	$\%\Delta\rho$	-5.3	-5.8
Moderator Temperature Coefficient	$X10^{-4}\Delta\rho/°F$	+0.5	-0.075
Fuel Temperature Coefficient Uncertainty	%	-15.0	0.0
Initial Axial Shape Index	asiu	0.0	0.0

TABLE C-7

SEQUENCE OF EVENTS
LOSS OF COOLANT FLOW EVENT
(BEST ESTIMATE)

Time	Event	Value
0.0	Loss of Power all Four Reactor Coolant Pumps	- -
1.0	Low Flow Trip	95% of initial flow
1.4	Trip Breakers Open	- -
1.75	CEAs Begin to drop into core	- -
4.0	Maximum RCS Pressure, psia	2257

TABLE C-8

KEY INPUT PARAMETERS ASSUMED IN THE SINGLE FULL LENGTH CEA DROP EVENT

Parameter	Units	Range of Values
Initial Core Power Level	% of 2710 MWt	100[+]
Initial Inlet Temperature	°F	548[+]
Initial RCS Pressure	psia	2225[+]
Initial Integrated Radial Peaking Factor F_r, Lead Bank Inserted 25%		1.693[+]
Initial Core Mass Flow Rate	$X10^6$ lbm/hr-ft^2	2.617[+]
Initial Axial Shape Index	asiu	-.2 to +.2[+]
CEA Drop Worth	$\%\Delta\rho$	-.08
Integrated Radial Peaking Factor Change	%	16.0
Moderator Temperature Coefficient	$X10^{-4}\Delta\rho$/°F	-2.5
Fuel Temperature Coefficient Multiplier		1.15

[+] Values quoted are without uncertainties. The uncertainties for these parameters were given in Table C-3.

TABLE C-9

SEQUENCE OF EVENTS
CEA DROP EVENT

Time (sec)	Event	Setpoint or Value
0.0	CEA Begin to Drop into Core	- -
1.0	CEA Reaches Full Inserted Position	100% Inserted
1.2	Core Power Level Reaches Minimum and Begins a Return to Power due to Reactivity Feedbacks	90.4% of Initial
100	Reactor Coolant System Pressure Reaches a New Steady State Value	2184
100	Core Power and Heat Flux Returns to its Maximum Value	100% of Initial

TABLE C-19

COMPARISON OF KEY INPUT PARAMETERS ASSUMED IN THE SAFETY ANALYSIS AND BEST ESTIMATE CASE FOR CEA DROP EVENT

Parameters	Units	Safety Analysis Values	Best Estimate Values
Initial Core Power Level	% of 2710 MWt	100.0	100.0
Initial Inlet Temperature	°F	548.0	548.0
Initial RCS Pressure	psia	2225	2225
Initial Integrated Radial Peaking Factor - Lead Bank Inserted 25%		1.693	1.59
Initial Core Mass Flow Rate	$X10^6$ lbm/hr-ft^2	2.617	2.617
Initial Axial Shape Index	asiu	-.08	-.08
CEA Drop Worth	%	-.08	-.13
Integrated Radial Peaking Factor Change	%	16.0	14.0
Moderator Temperature Coefficient	$X10^{-4}$ $\Delta\rho$/°F	-2.5	-3
Fuel Temperature Coefficient Multiplier		1.15	1.0

TABLE C-11

SEQUENCE OF EVENTS
CEA DROP EVENT
(BEST ESTIMATE)

Time (sec)	Event	Setpoint or Value
0.0	CEA Begin to Drop into Core	- -
1.0	CEA Reaches Full Inserted Position	100% Inserted
1.2	Core Power Level Reaches Minimum and Begins a Return to Power due to Reactivity Feedbacks	83.5% of Initial
40.6	Reactor Coolant System Pressure Reaches a Minimum Value	2172
103	Core Power Returns to its Maximum Value	99.5% of Initial
103	Core Heat Returns to its Maximum Value	99.5% of Initial

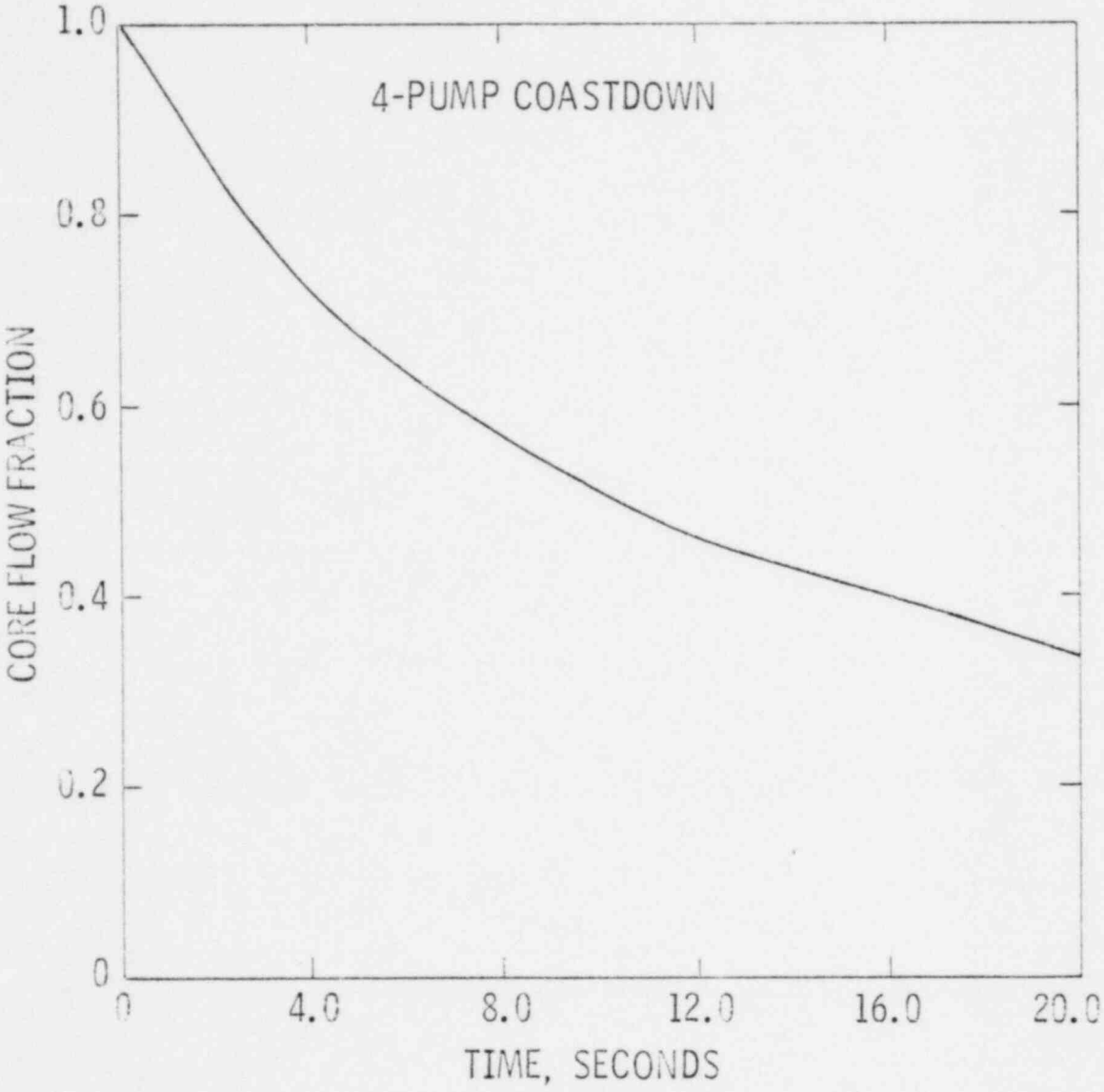

BALTIMORE GAS & ELECTRIC CO. Calvert Cliffs Nuclear Power Plant	LOSS OF COOLANT FLOW EVENT CORE FLOW FRACTION vs TIME	Figure C-1

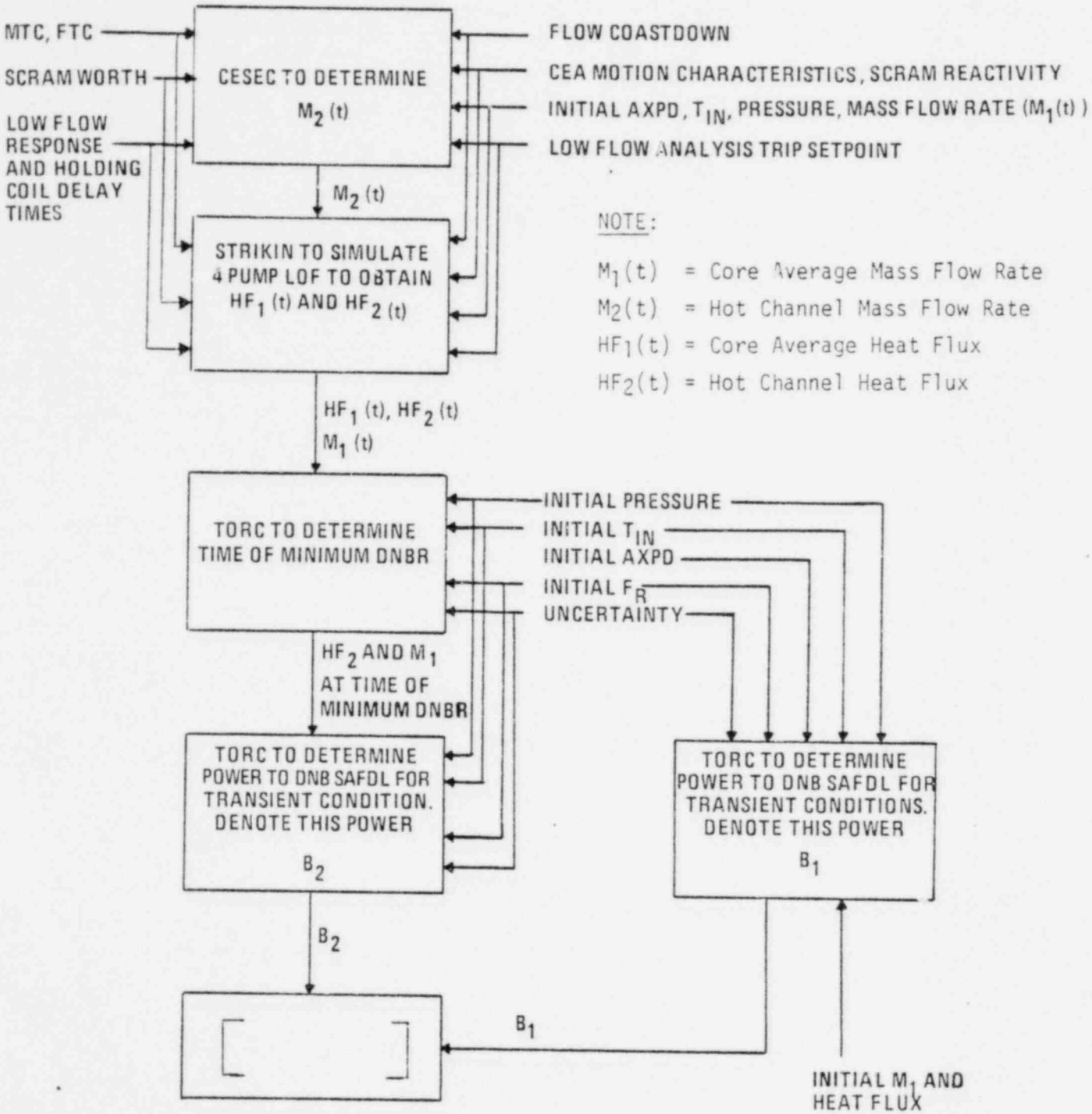

BALTIMORE GAS & ELECTRIC CO. Calvert Cliffs Nuclear Power Plant	PROCEDURES FOR LOSS OF COOLANT FLOW EVENT (STRIKIN - TORC METHOD)	Figure C-2

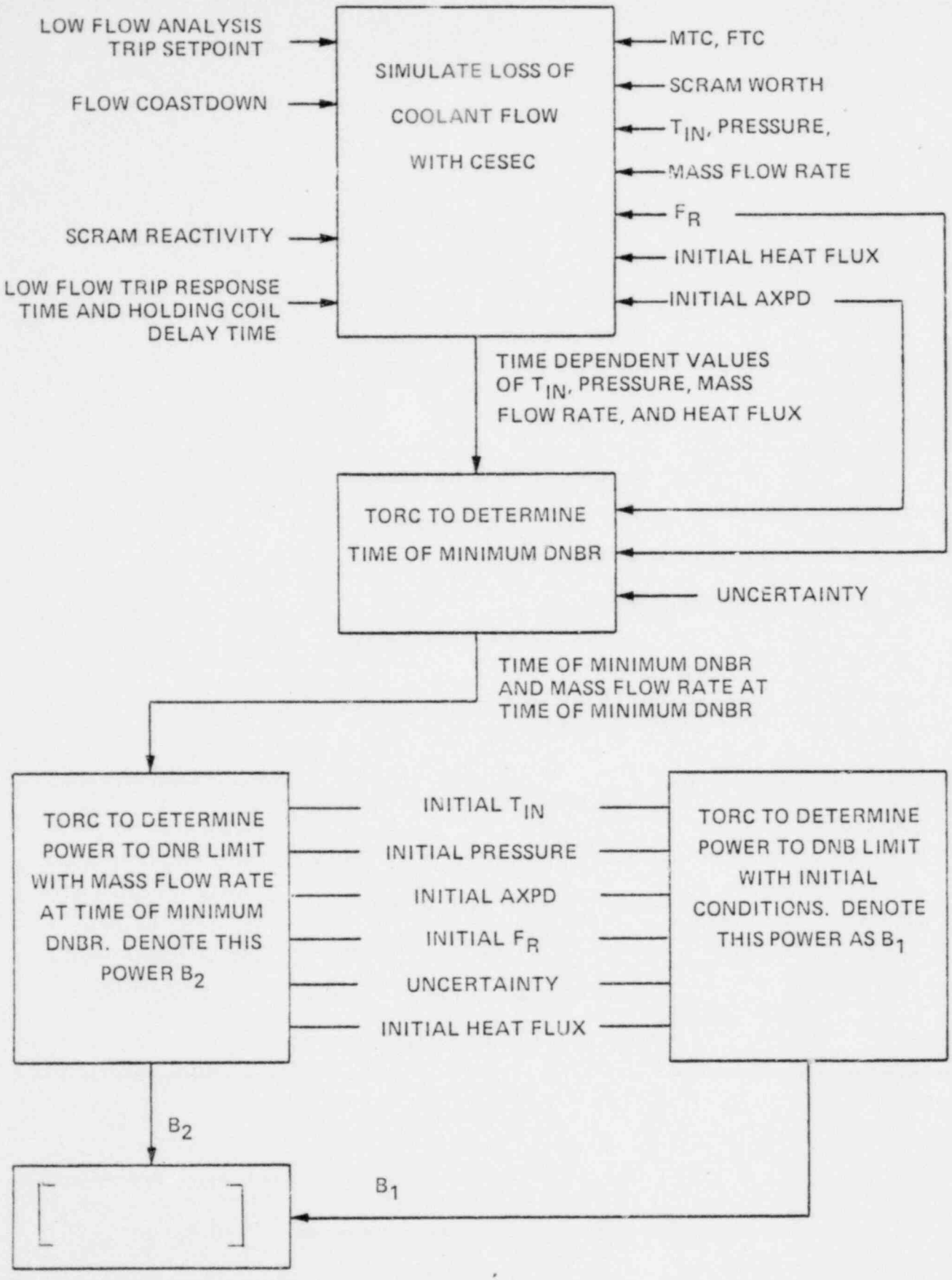

BALTIMORE GAS & ELECTRIC CO. Calvert Cliffs Nuclear Power Plant	PROCEDURES USED TO DETERMINE REQUIRED OVERPOWER MARGIN DURING LOSS OF COOLANT FLOW EVENT (CESEC - TORC METHOD)	Figure C-3

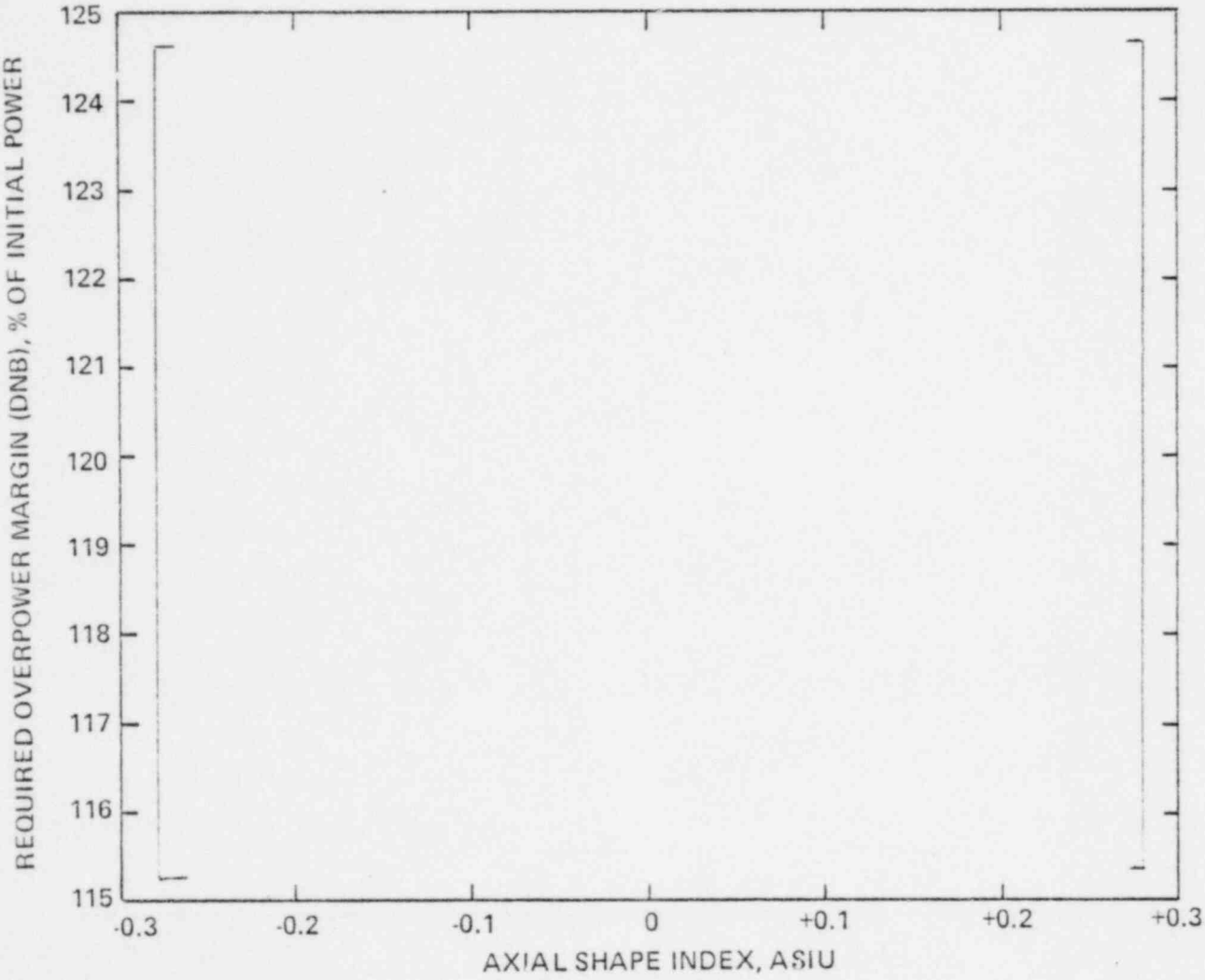

BALTIMORE GAS & ELECTRIC CO. Calvert Cliffs Nuclear Power Plant	LOSS OF COOLANT FLOW EVENT REQUIRED OVERPOWER MARGIN (DNB) AT 100% POWER vs AXIAL SHAPE INDEX	Figure C-4

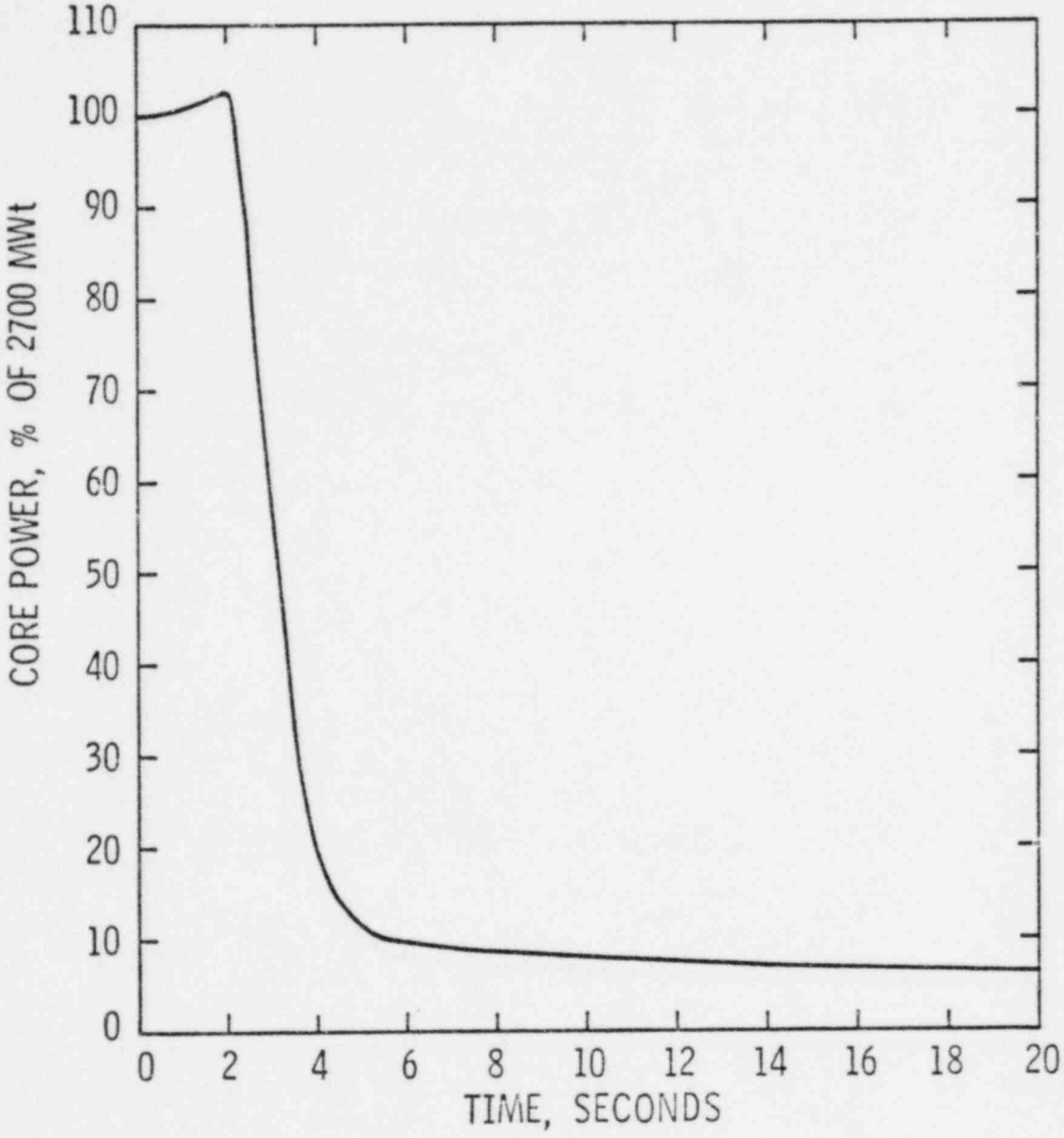

BALTIMORE GAS & ELECTRIC CO. Calvert Cliffs Nuclear Power Plant	LOSS OF FORCED COOLANT FLOW EVENT CORE POWER vs TIME	Figure C-5

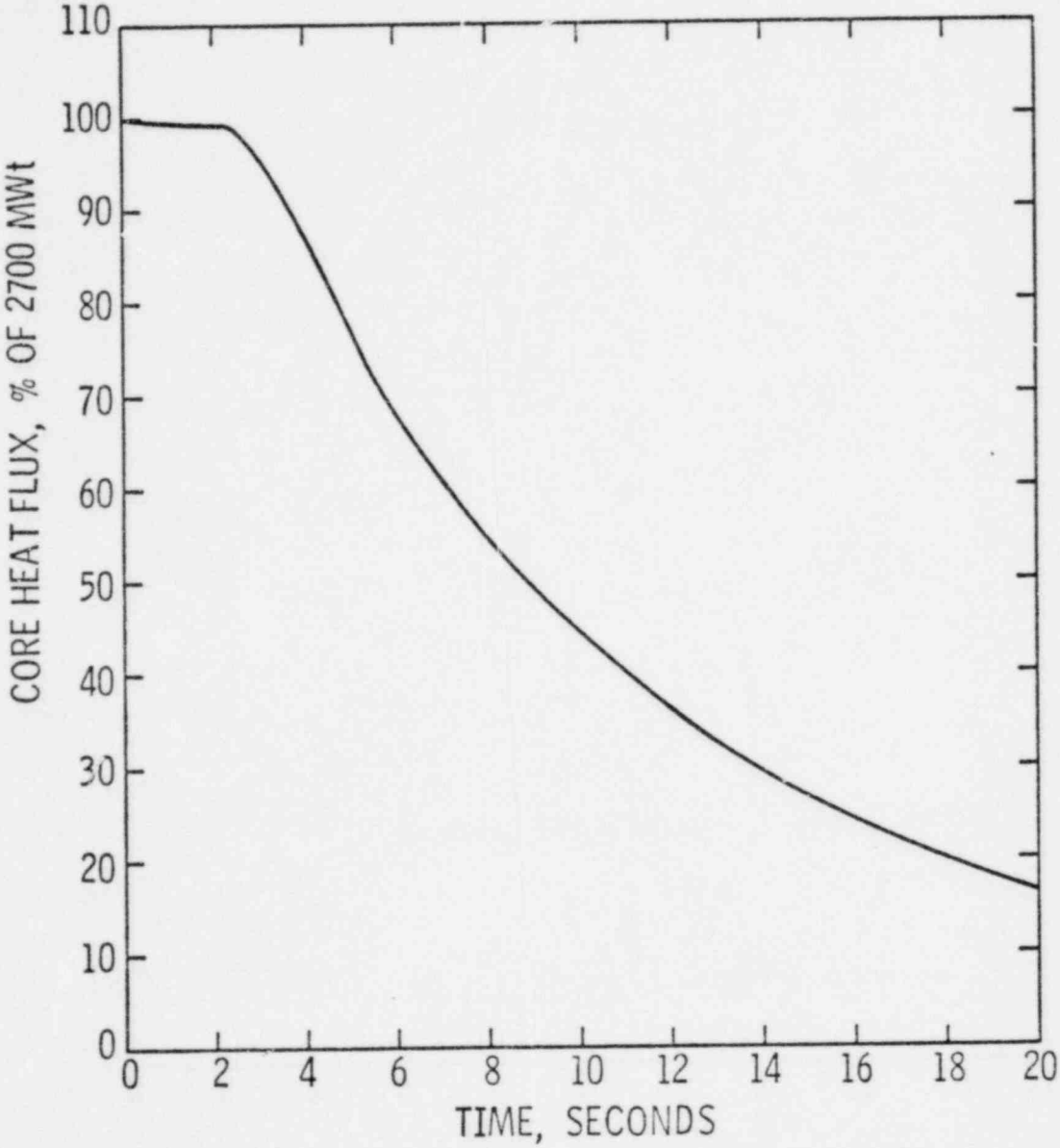

BALTIMORE GAS & ELECTRIC CO. Calvert Cliffs Nuclear Power Plant	LOSS OF FORCED COOLANT FLOW EVENT CORE HEAT FLUX vs TIME	Figure C-6

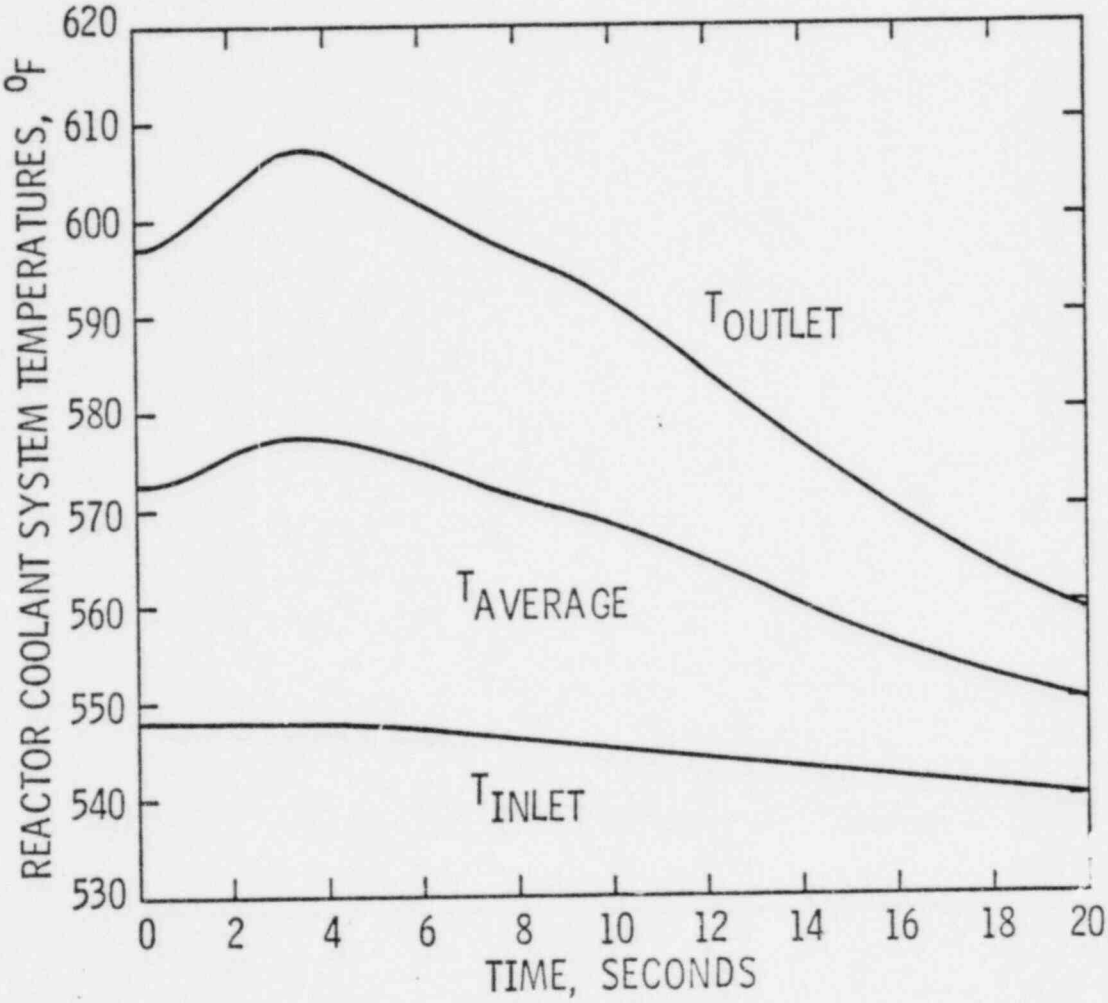

BALTIMORE GAS & ELECTRIC CO. Calvert Cliffs Nuclear Power Plant	LOSS OF FORCED COOLANT FLOW EVENT RCS TEMPERATURES vs TIME	Figure C-7

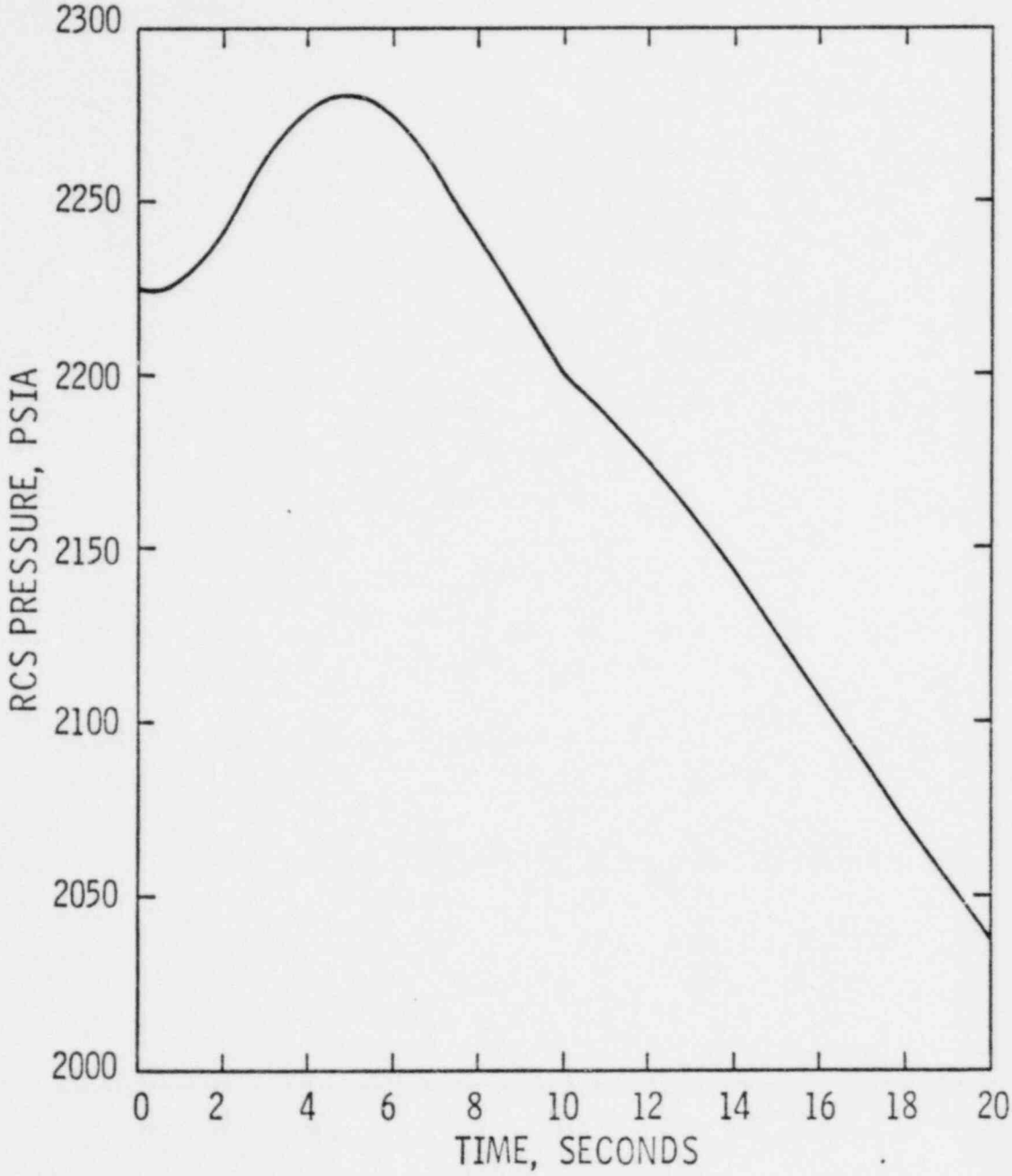

BALTIMORE GAS & ELECTRIC CO. Calvert Cliffs Nuclear Power Plant	LOSS OF FORCED COOLANT FLOW EVENT RCS PRESSURE vs TIME	Figure C-8

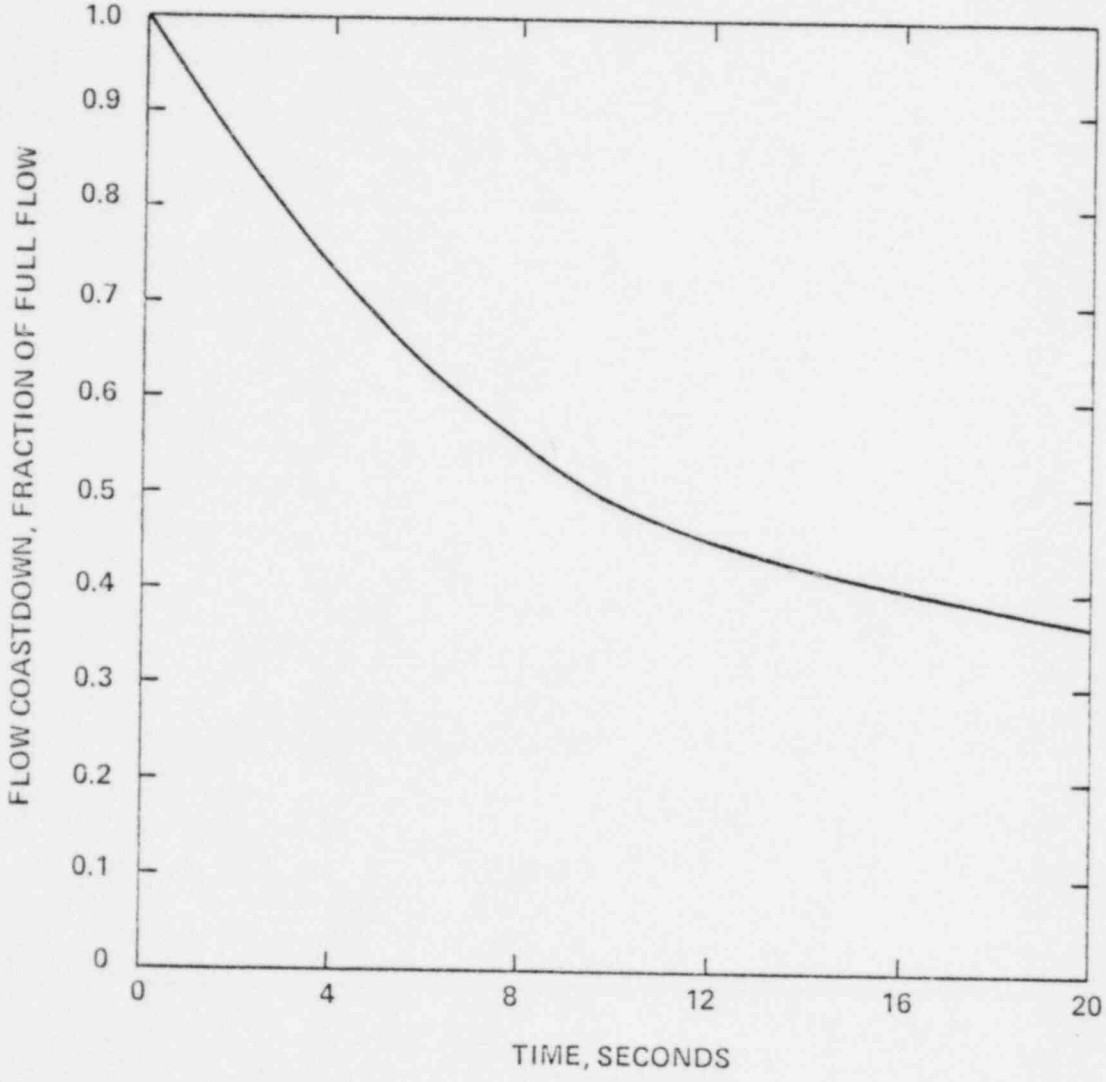

BALTIMORE GAS & ELECTRIC CO. Calvert Cliffs Nuclear Power Plant	LOSS OF COOLANT FLOW EVENT (BEST ESTIMATE) 4 PUMP FLOW COASTDOWN vs TIME	Figure C-9

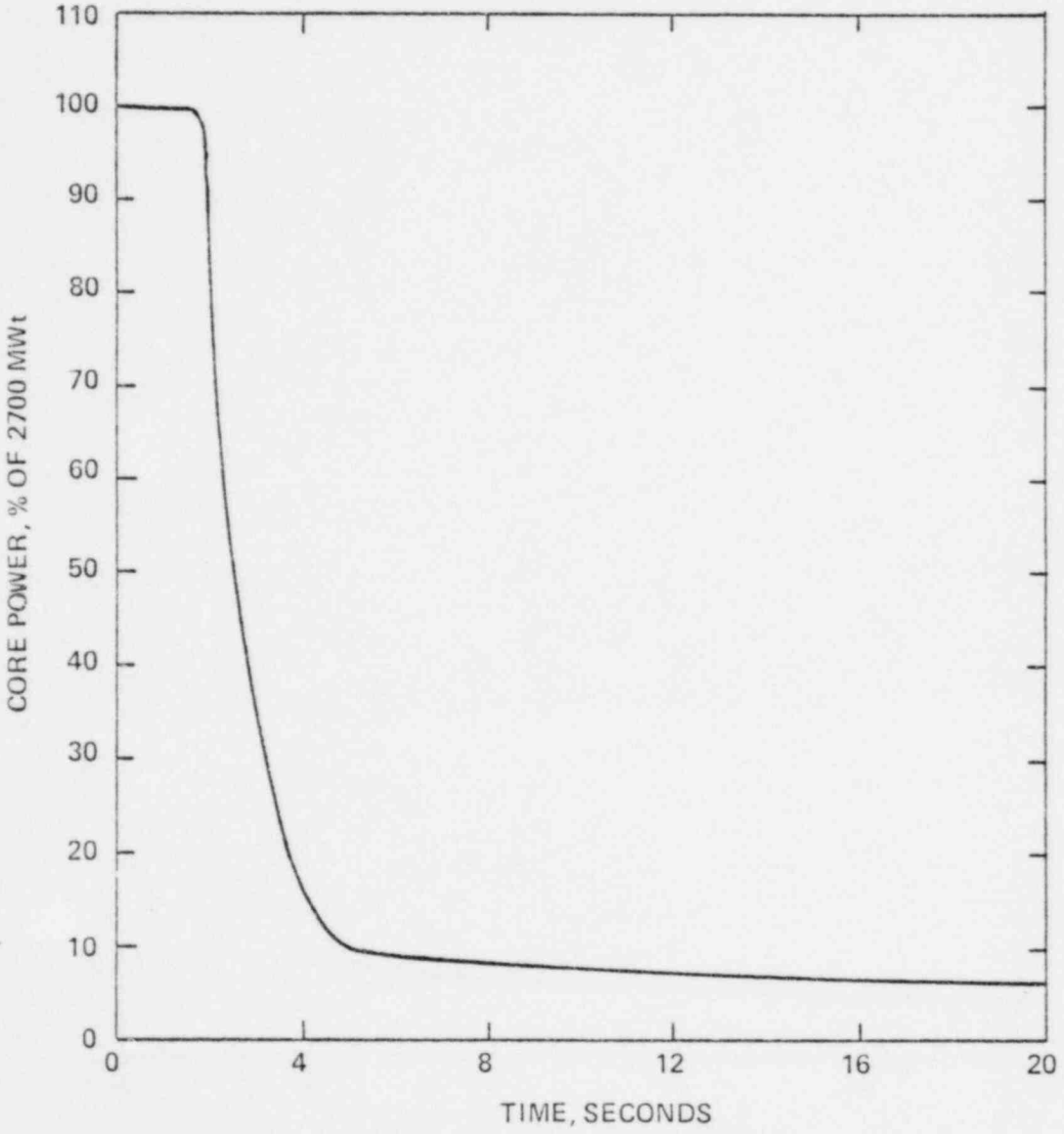

BALTIMORE GAS & ELECTRIC CO. Calvert Cliffs Nuclear Power Plant	LOSS OF COOLANT FLOW EVENT (BEST ESTIMATE) CORE POWER vs TIME	Figure C-10

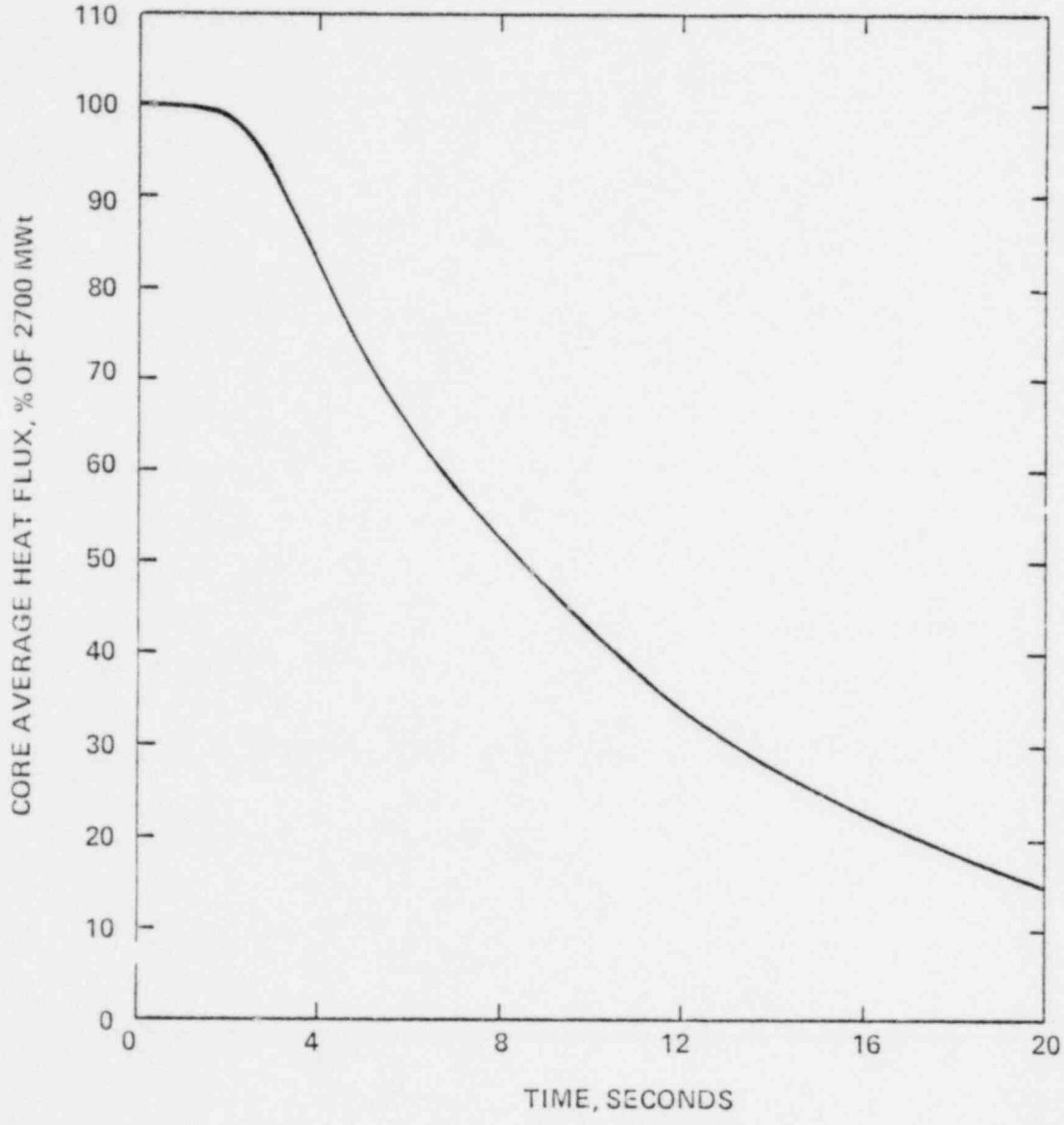

BALTIMORE GAS & ELECTRIC CO. Calvert Cliffs Nuclear Power Plant	LOSS OF COOLANT FLOW EVENT (BEST ESTIMATE) CORE AVERAGE HEAT FLUX vs TIME	Figure C-11

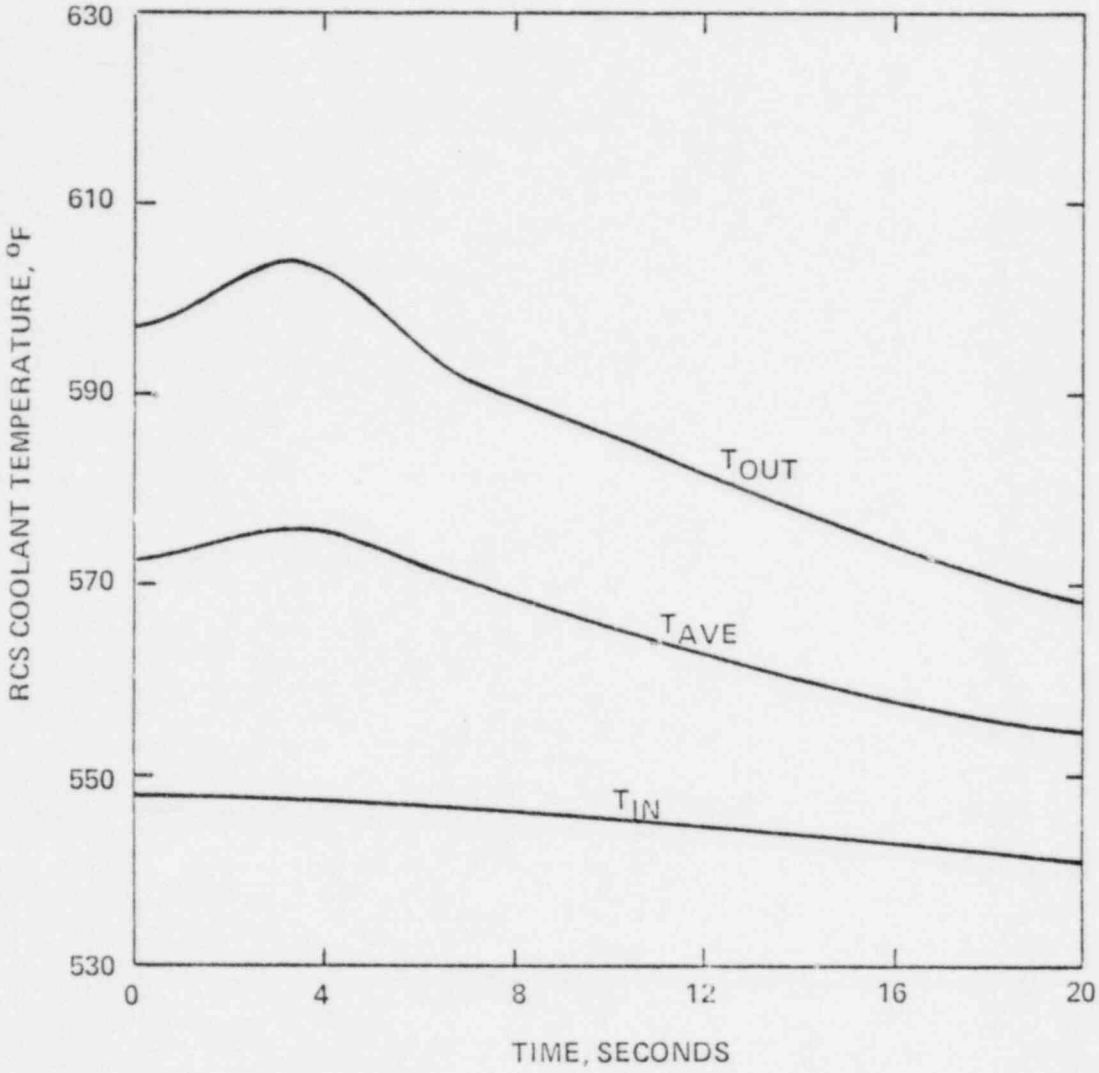

BALTIMORE GAS & ELECTRIC CO. Calvert Cliffs Nuclear Power Plant	LOSS OF COOLANT FLOW EVENT (BEST ESTIMATE) RCS COOLANT TEMPERATURE vs TIME	Figure C-12

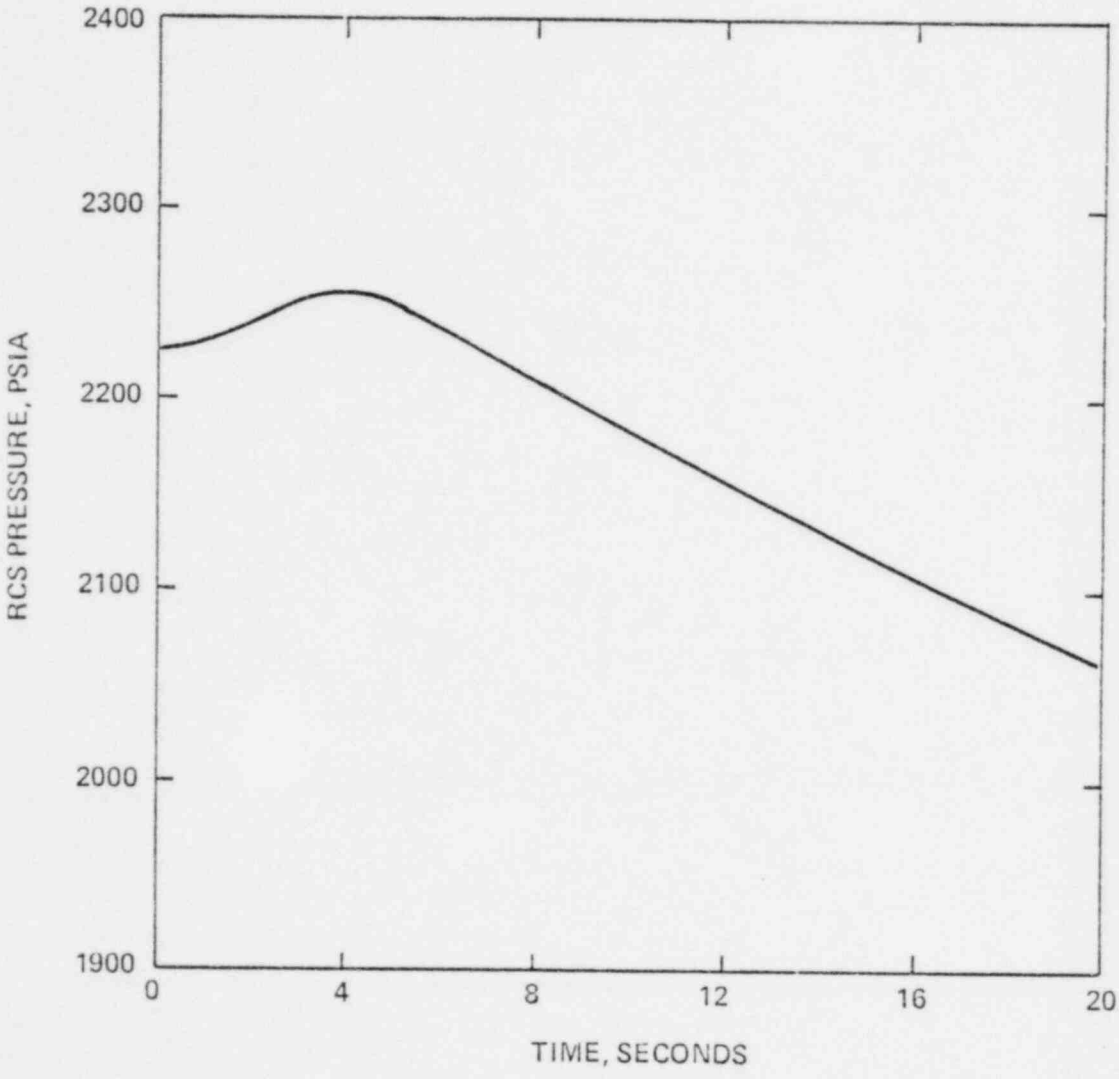

BALTIMORE GAS & ELECTRIC CO. Calvert Cliffs Nuclear Power Plant	LOSS OF COOLANT FLOW EVENT (BEST ESTIMATE) RCS PRESSURE vs TIME	Figure C-13

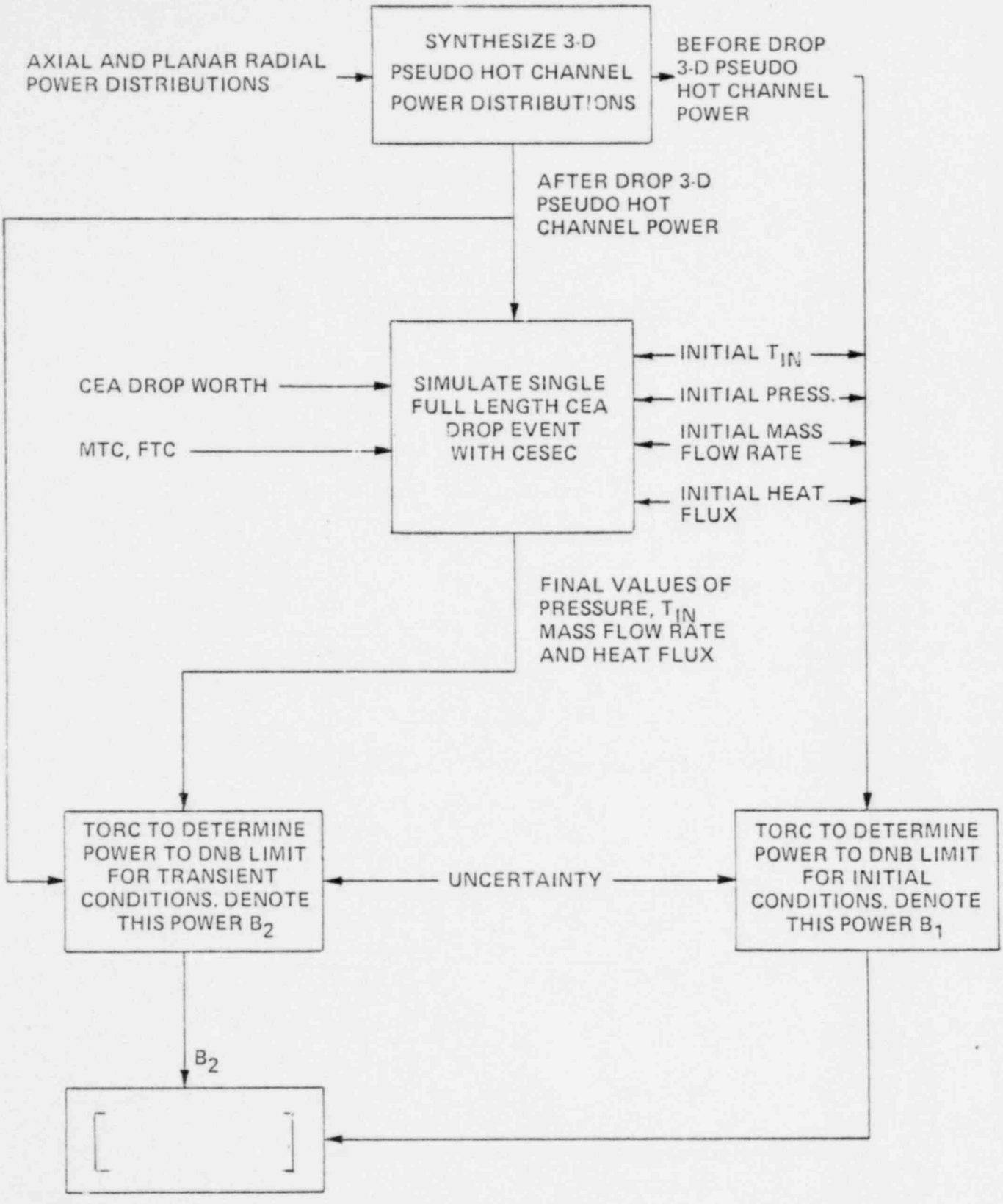

BALTIMORE GAS & ELECTRIC CO. Calvert Cliffs Nuclear Power Plant	PROCEDURES USED TO DETERMINE REQUIRED OVERPOWER MARGIN DURING SINGLE FULL LENGTH CEA DROP EVENT	Figure C-14

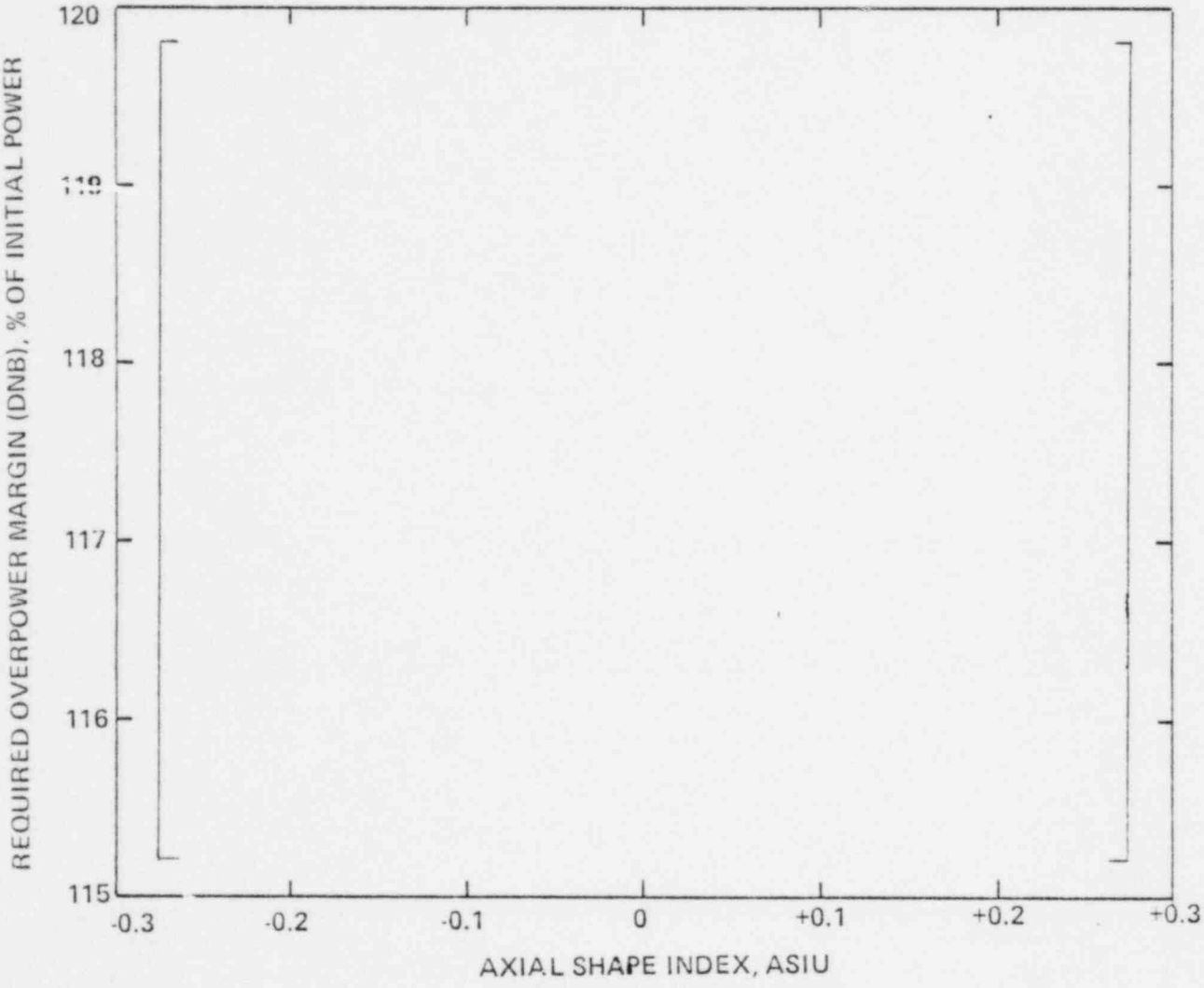

BALTIMORE GAS & ELECTRIC CO. Calvert Cliffs Nuclear Power Plant	CEA DROP EVENT REQUIRED OVERPOWER MARGIN (DNB) AT 100% POWER vs AXIAL SHAPE INDEX	Figure C-15

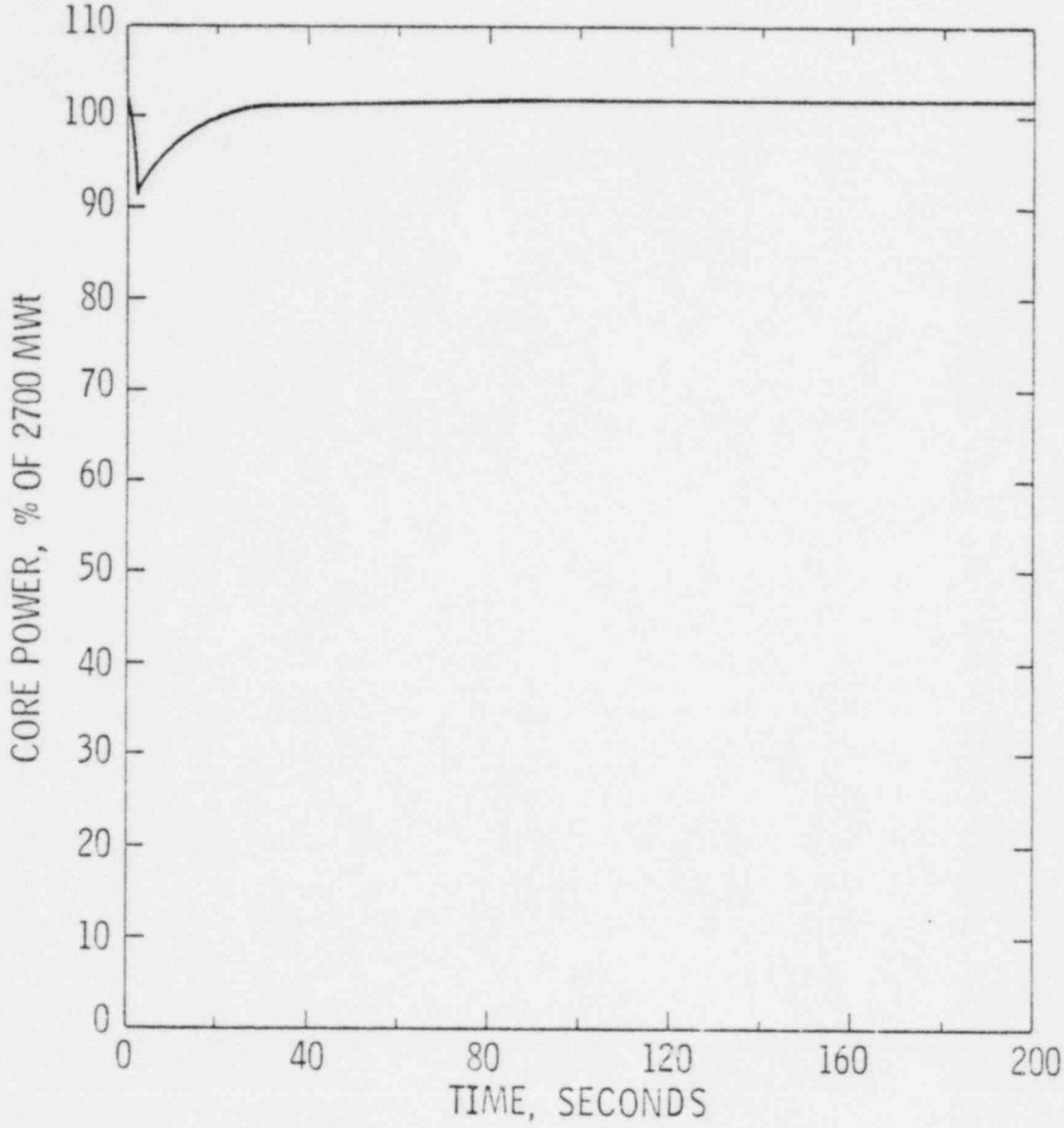

BALTIMORE GAS & ELECTRIC CO. Calvert Cliffs Nuclear Power Plant	SINGLE FULL LENGTH CEA DROP EVENT CORE POWER vs TIME	Figure C-16

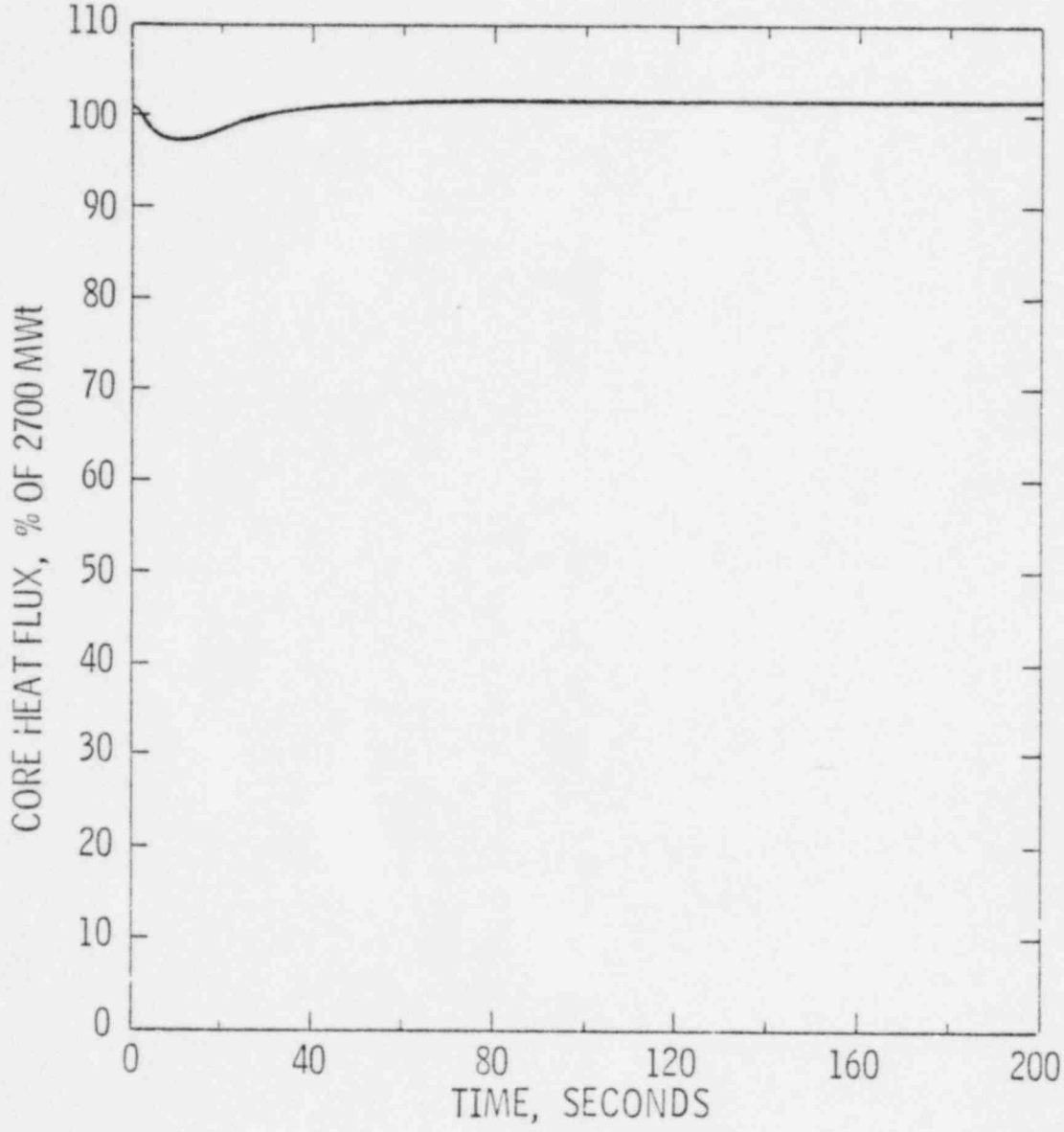

BALTIMORE GAS & ELECTRIC CO. Calvert Cliffs Nuclear Power Plant	SINGLE FULL LENGTH CEA DROP EVENT CORE HEAT FLUX vs TIME	Figure C-17

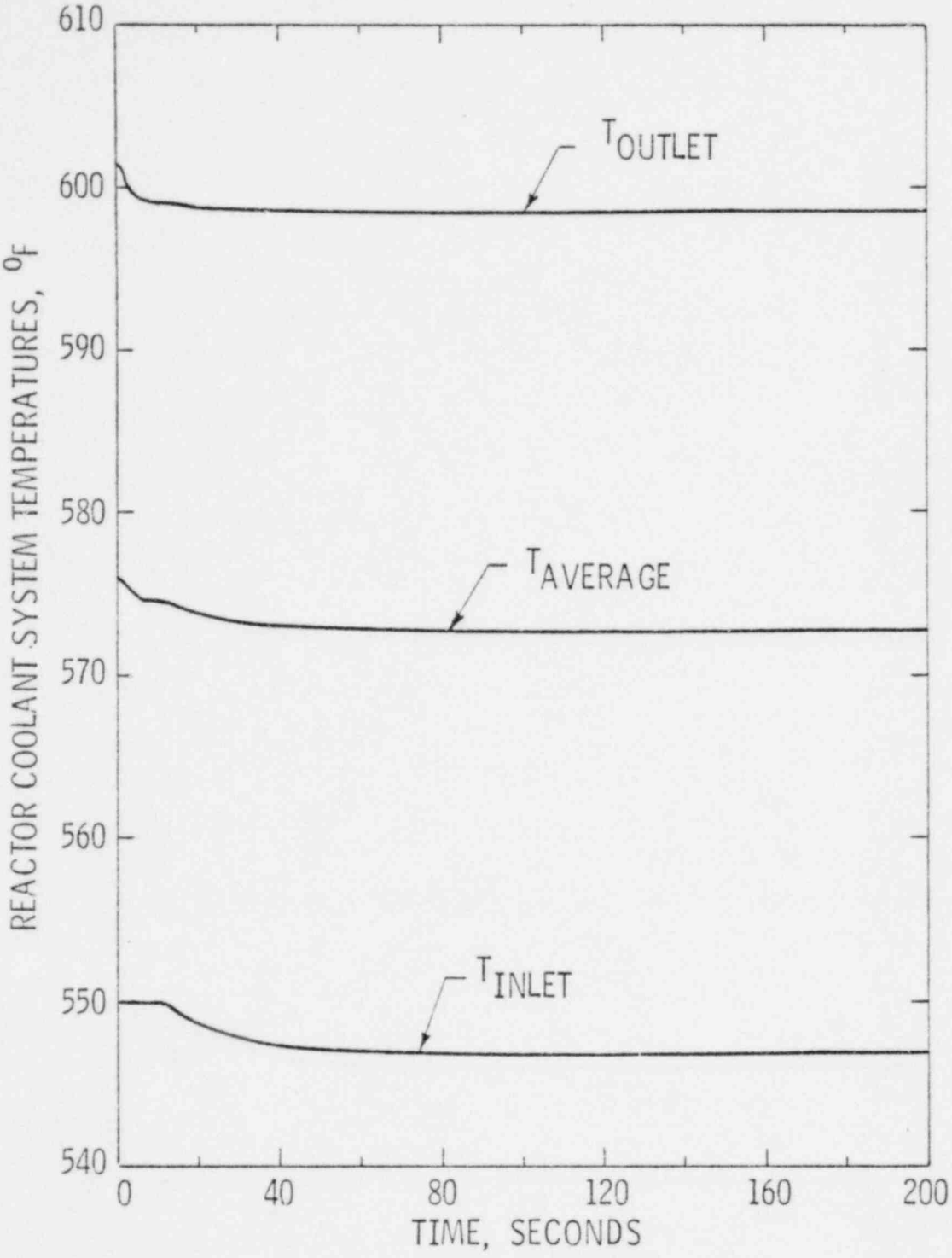

BALTIMORE GAS & ELECTRIC CO. Calvert Cliffs Nuclear Power Plant	SINGLE FULL LENGTH CEA DROP EVENT RCS TEMPERATURES vs TIME	Figure C-18

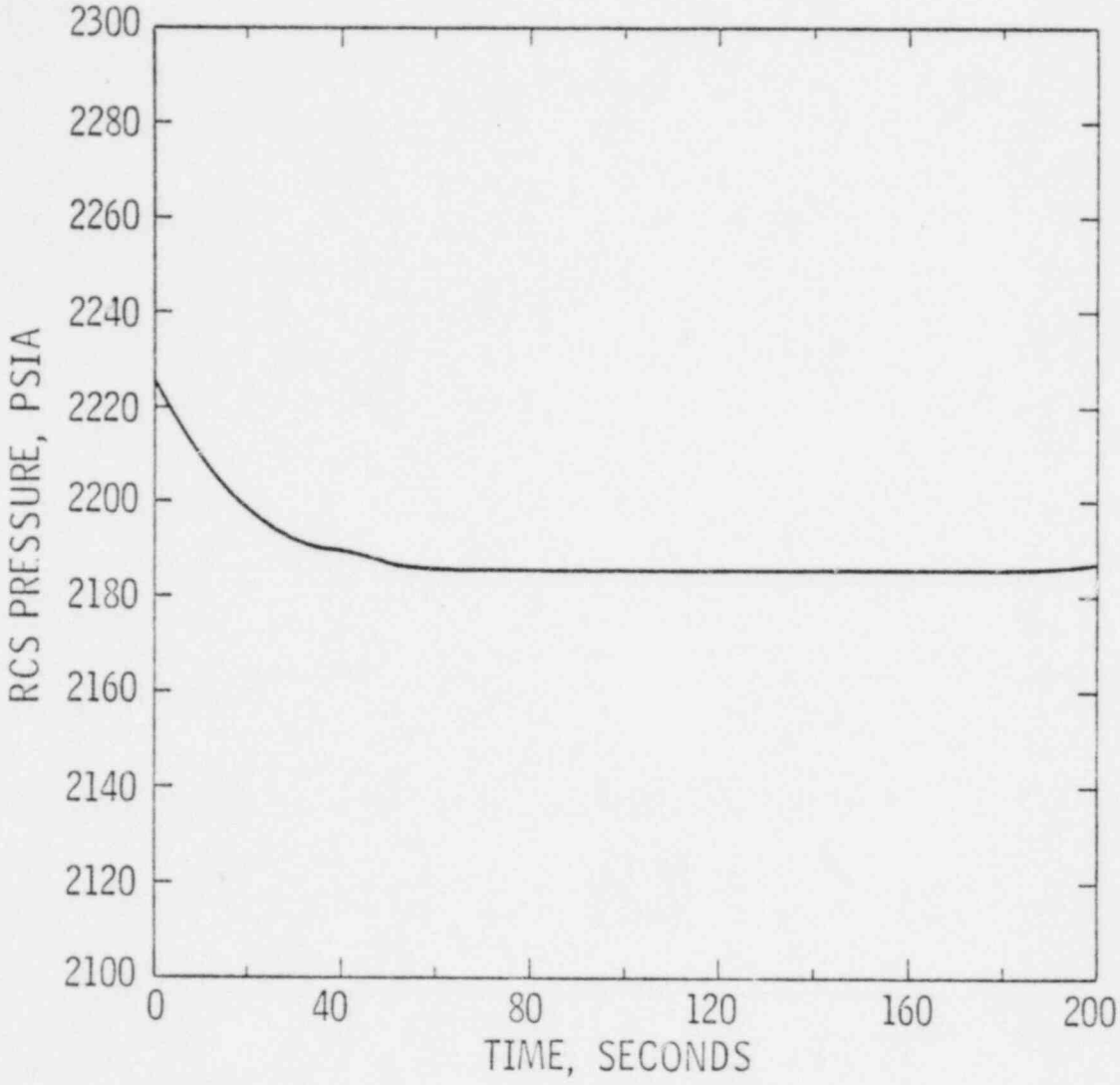

BALTIMORE GAS & ELECTRIC CO. Calvert Cliffs Nuclear Power Plant	SINGLE FULL LENGTH CEA DROP EVENT RCS PRESSURE vs TIME	Figure C-19

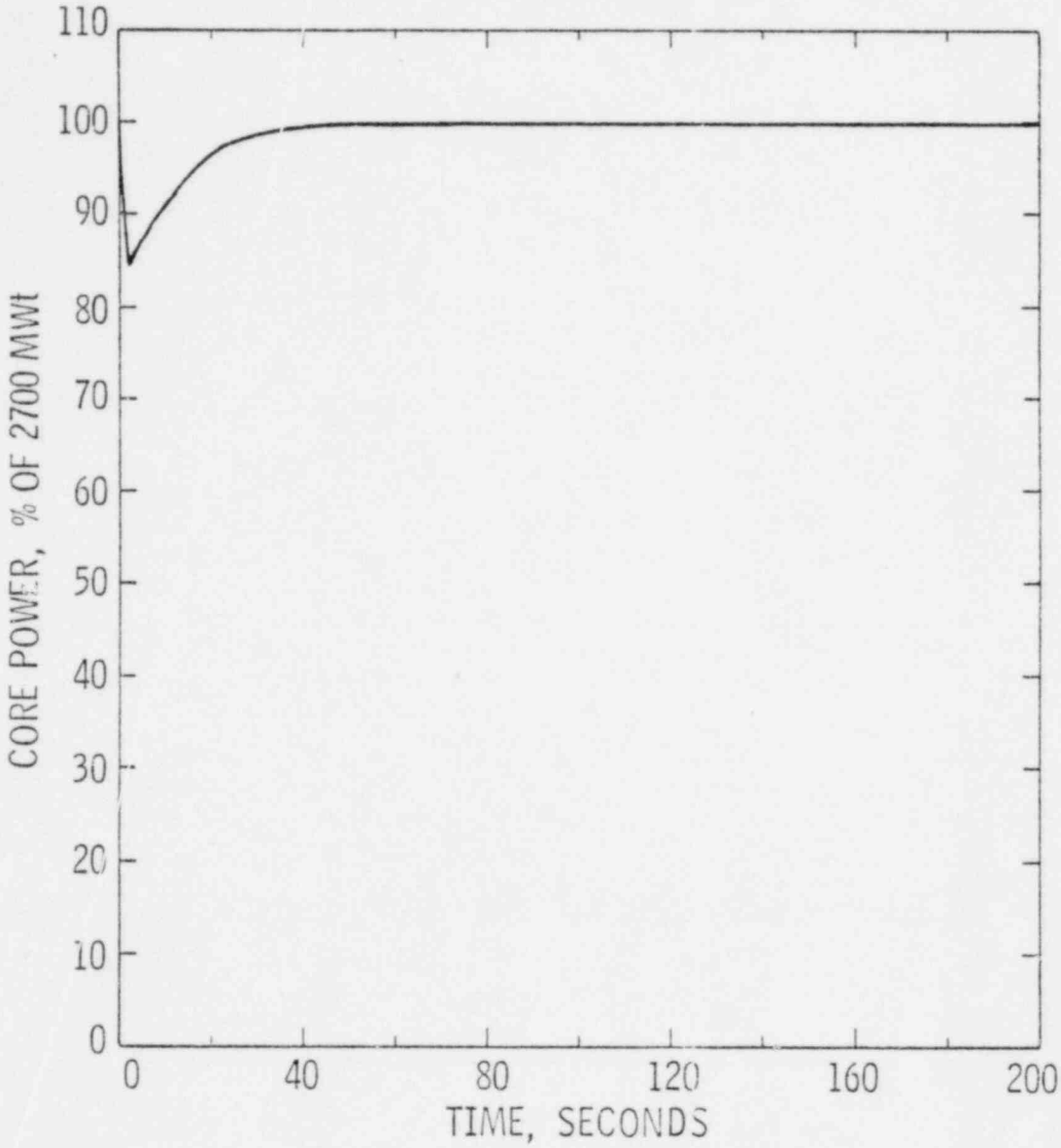

BALTIMORE GAS & ELECTRIC CO. Calvert Cliffs Nuclear Power Plant	SINGLE FULL LENGTH CEA DROP EVENT BEST ESTIMATE CORE POWER vs TIME	Figure C-20

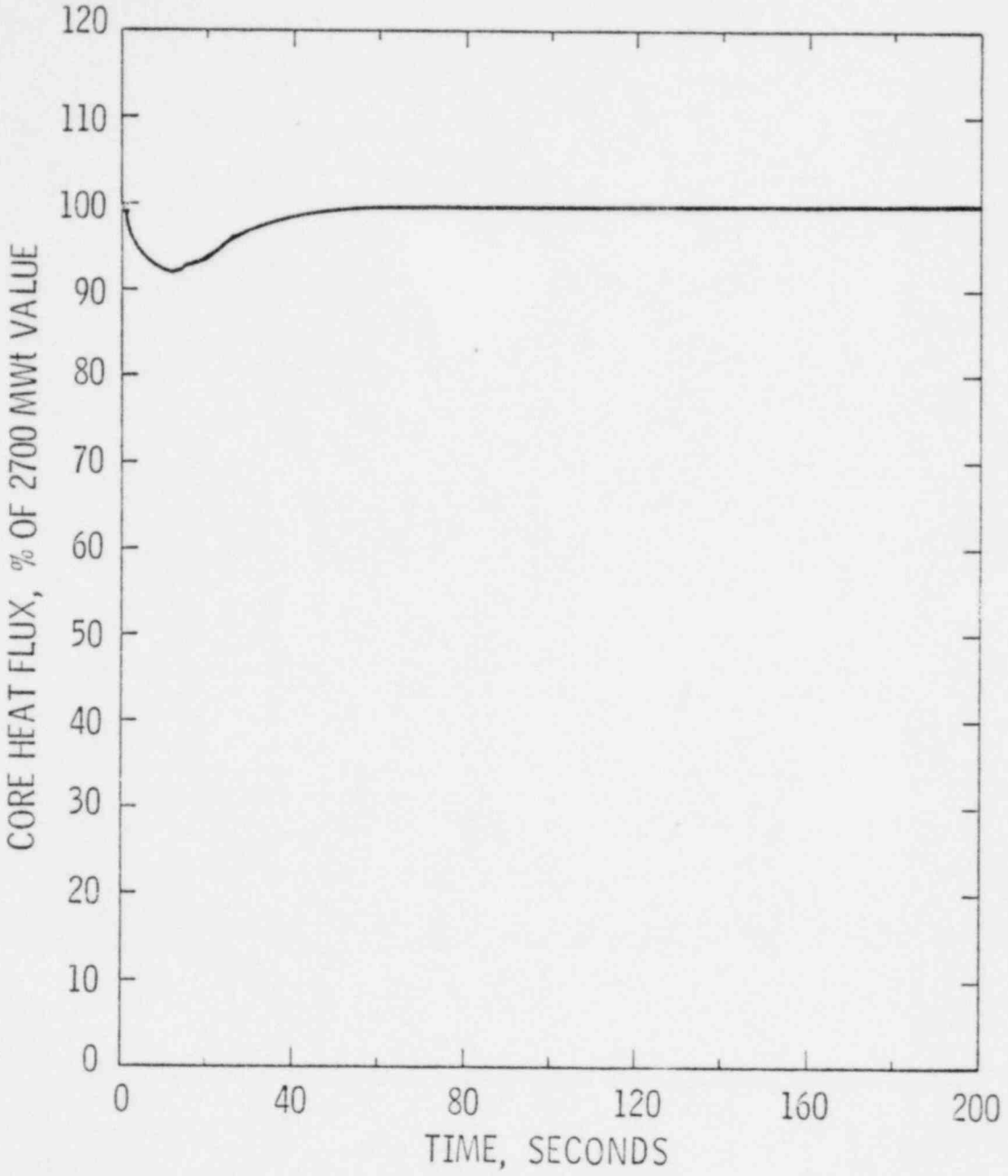

BALTIMORE GAS & ELECTRIC CO. Calvert Cliffs Nuclear Power Plant	SINGLE FULL LENGTH CEA DROP EVENT BEST ESTIMATE CORE HEAT FLUX vs TIME	Figure C-21

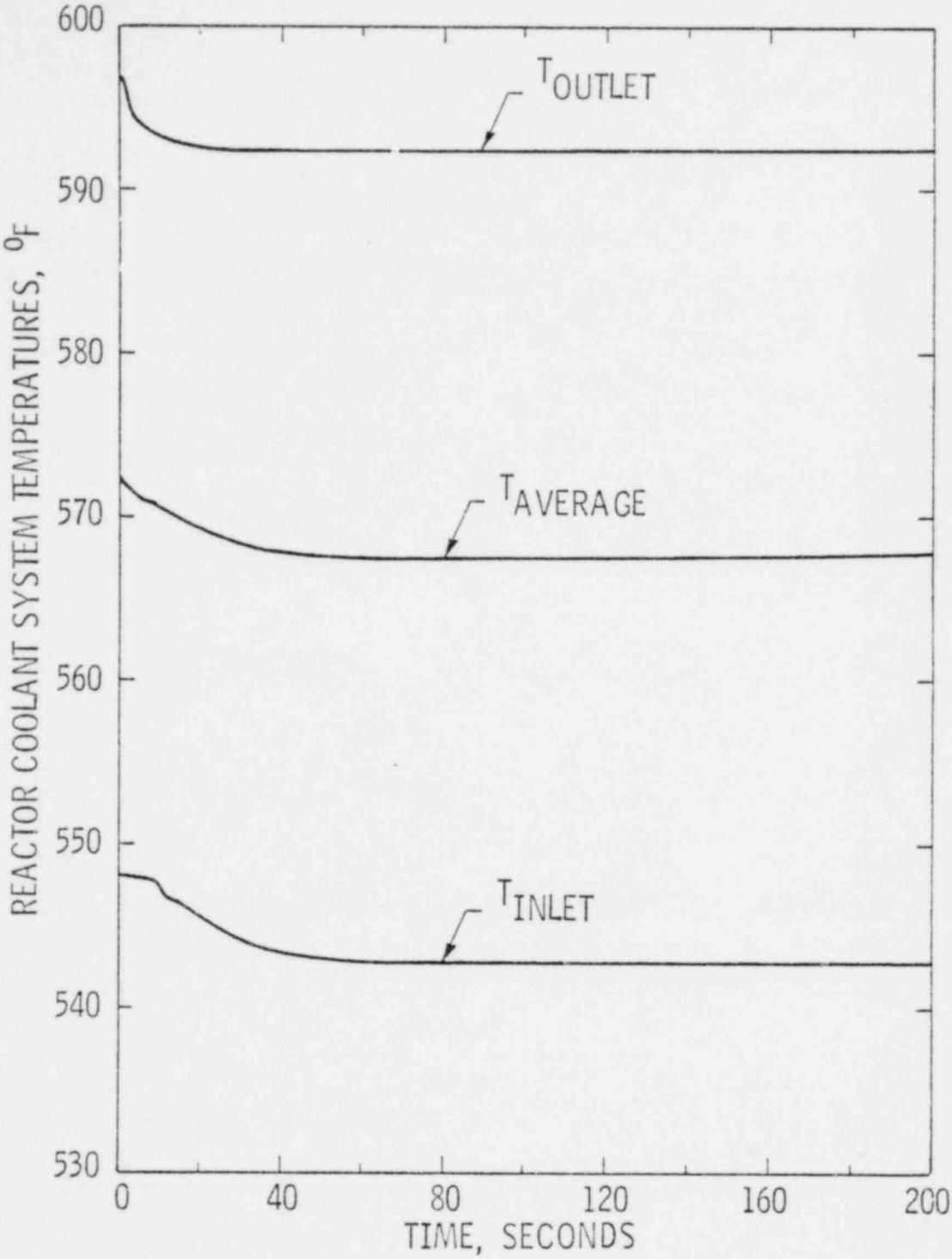

BALTIMORE GAS & ELECTRIC CO. Calvert Cliffs Nuclear Power Plant	SINGLE FULL LENGTH CEA DROP EVENT BEST ESTIMATE RCS TEMPERATURES vs TIME	Figure C-22

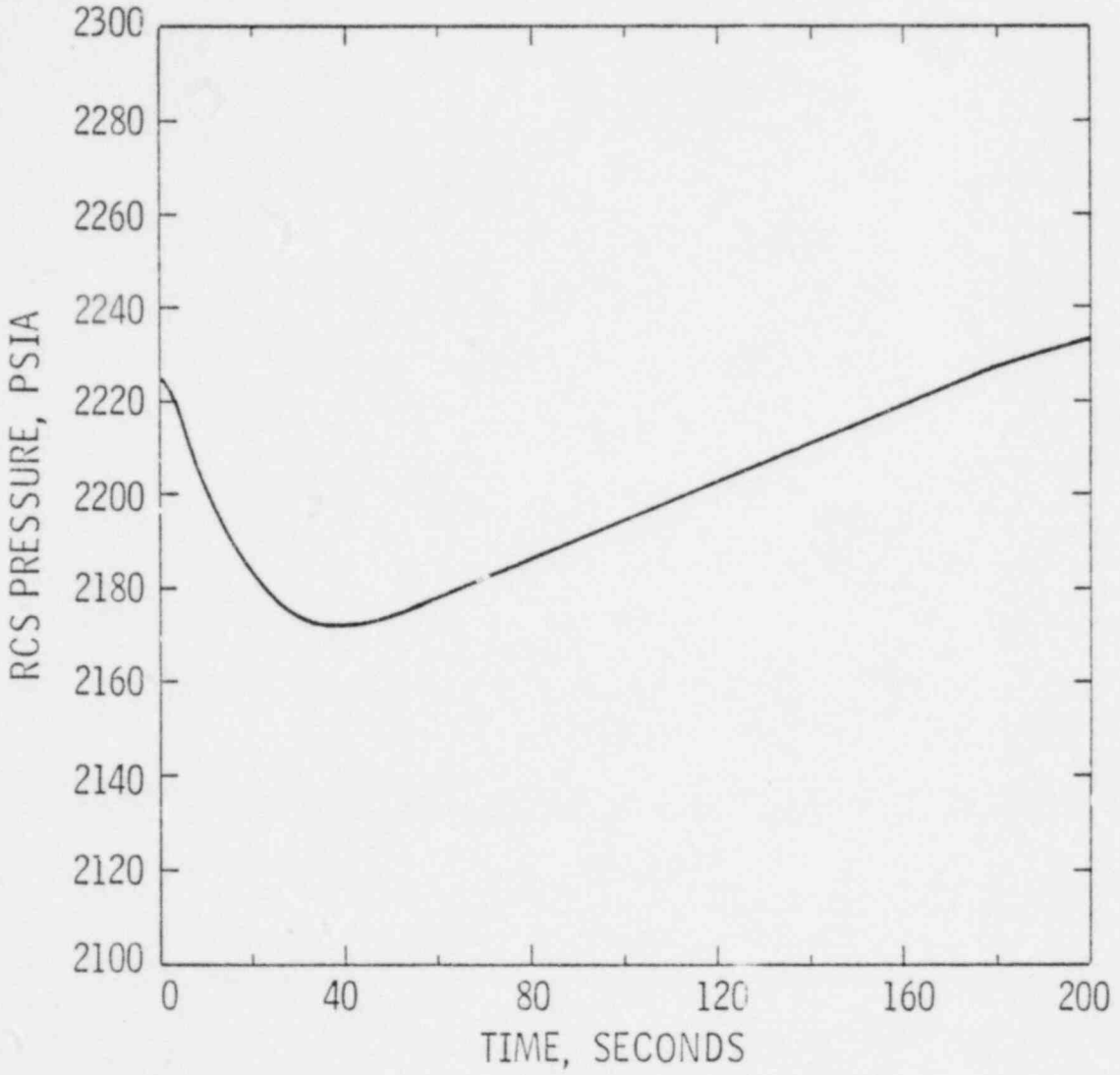

BALTIMORE GAS & ELECTRIC CO. Calvert Cliffs Nuclear Power Plant	SINGLE FULL LENGTH CEA DROP EVENT BEST ESTIMATE RCS PRESSURE vs TIME	Figure C-23